Sudan University of Science and Technology

College of Graduate Studies

Impact of Merowe Power Generation on the Performance of the Sudanese Electric National Grid

أثر توليد كهرباء سد مروي على أداء الشبكة القومية للكهرباء

A thesis submitted in partial fulfillment for the requirement of the degree of Master of Science in electrical engineering (power)

Prepared by:

Gafar Ali Elbashir

Supervised by:

Dr. Abdelaziz Yousif Mohamed Abbas

Apr, 2016

الآية

(اللَّهُ نُورُ السَّمَاوَاتِ وَالأَرْضِ مَثَلُ نُورِهِ كَمِشْكَاةٍ فِيهَا مِصْبَاحٌ الْمِصْبَاحُ فِي زُجَاجَةٍ

الزُّجَاجَةُ كَأَنَّهَا كَوْكَبٌ دُرِّيٌّ يُوقَدُ مِن شَجَرَةٍ مُّبَارَكَةٍ زَيْتُونَةٍ لَّا شَرْقِيَّةٍ وَلَا

غَرْبِيَّةٍ يَكَادُ زَيْتُهَا يُضِيءُ وَلَوْ لَمْ تَمْسَسْهُ نَارٌ نُّورٌ عَلَى نُورٍ يَهْدِي اللَّهُ لِنُورِهِ مَن يَشَاء

وَيَضْرِبُ اللَّهُ الأَمْثَالَ لِلنَّاسِ وَاللَّهُ بِكُلِّ شَيْءٍ عَلِيمٌ)

صدق الله العظيم

سورة النور آية رقم (35)

Dedication

In memory of my honorable teacher the late Hashim Ibrahim Sheban, the exemplary role model whose lasting impact remains the greatest on the development of my (and my contemporaries') positive attitudes towards hard work . Patience and love lifelong learning.

Acknowledgments

Thanks to Allah the compassionate the merciful for giving me patience and strength to accomplish this research

All thanks and appreciations go to Allah for His unlimited blessings and for giving me the strength to complete this study.

Special thanks are extended to my supervisor Dr. **Abdelaziz Yousif Mohamed Abbas** for his considerable effort, great help and continuous scientific directing along this study.

My appreciation is also extended to the Sudan University of Science & Technology for giving me the opportunity to carry out this study. Furthermore, great thanks are also to my colleagues and lecturers in the Engineering Faculty and the Electrical Engineering Department in particular for their continual encouragement and support.

Thanks go to ministry for water resource, irrigation and Electricity , for providing me all the necessary information that was helpful in accomplishing this work.

Finally, my most appreciations are to my parents, wife, daughters, brothers and sisters

For their full support, encouragement and patience that give me the power all life.

ABSTRACT

The Sudanese National Grid suffered severe supply shortages prior to Merowe. The advantages and challenges arising from the introduction of Merowe power are addressed here. Power-flow, short circuit, contingency and stability analyses of the National Grid are presented for both before- and after-Merowe cases. Comparisons are drawn between the two cases to show system improvement and propose solutions to observed challenges. The analyses show system improvement in terms of adequacy of supply, enhancement in stability and significant reduction of the need to apply load shedding as well as N-1 criteria, transient stability and voltage profile. Proposals are made to improve transmission network performance through increasing transmission capacity and installing SVCs at carefully selected locations. Proposals are also made to increase network components capacities to maintain N-1 stability criteria in the future. Distributed generation, particularly in Khartoum is recommended as a means of addressing forecasted generation shortages. In addition, it is proposed that other plants comparable to Merowe in generation capacity be incorporated at other locations to avoid instability risks that may result from loss of Merowe at any time.

ملخص البحث

ظلت الشبكة القومية للكهرباء قبل دخول محطة توليد مروي الخدمة تعاني من عجز في التوليد ، جراء التمدد في استخدامات الكهرباء وللزيادة الافقية والراسية في الاحمال والتي لم تقابلها زيادة في التوليد بنفس القدر. هذا البحث ينظر في الميزات والتحديات بعد دخول مشروع سد مروي الخدمة ، قمنا بتحليل وضع الشبكة قبل وبعد دخول مروي الخدمة من خلال دراسة انسياب الاحمال وقصر الدائرة واعتمادية واستقرارية الشبكة، ورصد التحسن الكبير الذي طرأ علي الشبكة وكذلك التحديات التي يمكن ان تواجه الشبكة في المستقبل . تم دراسة مكونات الشبكة بعد التغير الذي حدث والزيادة والكبيرة في التوليد التي اضيفت وانعكاس ذلك علي اداء مكونات الشبكة واعتماد البدائل في حالة خروج معدة من الخدمة ، ودراسة وضع الجهود في كل الحالات . تم وضع مقترحات لتحسين اداء الشبكة بزيادة سعات مواعين النقل وباضافة معوضات القدرة غير الفعالة SVC مع تحديد المواقع المناسبة لها . ايضا اضافة توليد في ولاية الخرطوم باعتبارها اكبر مركز احمال في الشبكة ولمقابلة الزيادة الكبيرة والمستمرة للاحمال فيها . اضافة سعات توليد باحجام توازي توليد مروي ويراعي توزيع مواقعها لضمان استقرارية الشبكة وكذلك لمقابلة الطلب .

Table of Contents

Title	page
الآية	i.
Dedication	ii.
Acknowledgments	iii.
Abstract	iv.
ملخص البحث	vi.
Table of Contents	vii.
Table of figure	x.
CHAPTER ONE INTRODUCTION and BACKGROUND STUDIES	
1.1General Background ……..	1
1.2 Problem Definition and Objectives……	2
1.3 Motivations……	2
1.4 Methodology…….	3
1.5Thesis Layout…….	3
CHAPTER TWO THE SUDAN NATIONAL GRID	
2.1 Historical Background……..	4
2.2 Existing Power System……	4
2.3 National Grid Existing Generation Plants…….	5
2.3.1 Thermal Power Stations……..	5
2.3.2 Hydro Power Stations……	6
2.4 Existing Transmission Networks……..	6
2.5 Sudan National Grid Load Curve……..	7
CHAPTER THREE POWER SYSTEM MODELLING and CONTROL	
3.1 Introduction …….	9
3.2 Dynamics of Synchronous Machine…….	11
3.3 The Swing Equation……..	13
3.4 Multi –machine System……	15
3.5 Machines Swinging Coherently ……	15
3.6 Simplified Machine Model……..	16
3.7 Power Angle Curve for a Two Machine System…….	17
3.8 Two-Machine to One – machine – Infinite- Bus bar System …….	19
3.9 Transient Stability Analysis…….	19
3.10 Equal Area Criterion……..	21
3.11 Power system Control……..	27
3.12 Dynamic Performance Measures……	35

3.13 Governor- Turbine System……. 37
3.14 Static VAR Compensator (SVC) ……... 49
CHAPTER FOUR ANALYSIS of SUDAN NATIONAL GRID BEFORE and AFTER MEROWE DAM
4.1 Introduction ……. 52
4.2 Load Flow Analysis Theoretical Background …… 53
4.3 Grid Analysis ……. 57
CHAPTER FIVE CONCLUSIONS and RECOMMENDATIONS
5.1 Conclusion…….. 62
5.2 Recommendations…….. 63
References 65
Appendixes

Table of figure

Figure	Topic	Page
(3.1)	The torque, speed and flow of mechanical and electrical powers in a synchronous machine	14
(3.2)	The phasor diagram corresponding	18
(3.3)	The machine model corresponding	18
(3.4)	Power Angle Curve for a Two Machine System	19
(3.5)	Equal Area Criterion	23
(3.6)	Consider a single machine feeding an infinite busbar through a transmission link	24
(3.7)	the point ain the power angle diagram	25
(3.8)	The maximum possible value for δ2 is obtained as δmax	26
(3.9)	a single machine tied to an infinite bus through two parallel lines	26
(3.10)	the Plots of the power angle curves for the three cases	27
(3.11)	Is a simplified schematic diagram of a typical dc excitation systeı with an amplidyn voltage regulator.	29
(3.12)	the model of an IEEE typeDC1Aexcitation system	29
(3.13)	the excitation control when the generator is on open circuit	30
(3.14)	The DC Exciter Model	31
(3.15)	Illustrates a field controlled alternator rectifier system.	32
(3.16)	Illustrates an alternator supplied controlled rectifier system.	33
(3.17)	The third AC system shows a typical brushless excitation system	33
(3.18)	The AC exciter model	34
(3.19)	Static Excitation Systems	35
(3.20)	Small Signal Performance Measures	36
(3.21)	An open-loop frequency response characteristic of an excitation control system with generator open-circuited	37
(3.22)	The corresponding closed-loop frequency response with the generator open-circuited.	38
(3.23)	The (AGC) basic function blocks	39
(3.24)	Hydraulic Turbines characteristics	40
(3.25)	the governor turbine system	44
(3.26)	shown An improvement in stability is achieved by including a transient droop R_T characteristic in addition to the normal permanent droop R.	45
(3.27)	shown the (PID) action	46
(3.28)	Steam Turbines	47
(3.29)	Steam Vessel Modeling	48

(3.30)	The control valves are usually of the plug-type with characteristics as shown below in	49
(3.31)	A block diagram representation of a steam turbine system	50
(3.32)	A single-line diagram of a static VAR compensator	52
(3.33)	SVC Characteristics	53
(4.1)	The General Busbar	56

CHAPTER ONE

INTRODUCTION

1.1 General Background

Power systems are large networks designed to generate, transmit and distribute electric power to consumers to operate their electric devices, machines and appliances. Electric energy is usually converted to other forms of energy, such as light, heat, and mechanical energy for end use. Power is usually transmitted in AC form at high voltage via overhead power lines. The generating plants and the transmission network including power lines, substations and related equipment are referred to as the Grid. The performance of the Grid can be measured in different ways but can generally be viewed as the ability of the network to maintain affordable and reliable high quality supply around the clock despite the continuous changes in operating conditions and in the face of inherent and induced disturbances. The economic and reliable operation of power grids is a complex task that requires delivering generated power almost instantaneously, which explains the need to maintain a balance between demand and generation at all times. Normal operating condition is referred to as steady state operation which means that generators, lines and transformers are operated within their limits and bus voltages are kept at or very close to their rated values.

The Sudanese Grid before Merowe, as described in detail in chapter two, consisted of three thermal plants and four hydropower plants with a total available capacity of 800 MW. Thermal plants contributed about 60% of the total capacity while the hydropower plants contributed the remaining 40%. The transmission network, also described in detail in chapter two, consisted of 110, 220 and 66 kv transmission lines. The 220kv double circuit transmission system runs about 500 km from Roseires substation in Blue Nile State to KiloX substation in Khartoum State with several substations in between. The

110 kv system consisted of a 70 km ring around Khartoum, a line from Sennar substation to KiloX substation (in Khartoum) via Hag Abd Alla Maringan, Hasahesa, Giad and El Bagir substations and a line from Maringan substation to Gadaref substation via Fau substation. The 66 kv transmission network runs from Girba to Kassala and from Girba to Gadaref where it is connected to the national grid via the 110 kV line coming from Maringan substation via Fau substation.

1.2 Motivations

Merowe Project was a huge undertaking that resulted in a huge unprecedented addition to the electric power system of the Sudan. This project comprises the largest power plant in the Grid. The individual generation units are also the largest in the system thus, making Merowe the leading power generating plant. These features in addition to the state of the art high quality unit control systems that characterize Merowe Plant added generation capacity and also lead to an overall positive impact in terms of better stability and improved performance of the entire system Nevertheless, the plant location is far from load centers giving rise to voltage drop issues. Merowe –Markhiat transmission lines are fitted with reactors that are constantly in operation. All of the above makes it interesting and necessary to study the impact, positive or negative, of Merowe Plant on the Sudanese Power Grid.

1.3 Objectives

The work presented in this dissertation aims to provide a study of the impact of the implementation of the Merowe Dam Project on the Sudanese National Grid performance. Merowe project provides a potential increase in generation capacity of 1250 MW of hydro power and added transmission capacity to deliver this power to the load centers around the country. The Grid before Merowe is examined to provide contrast and means for comparison.

1.4 Methodology

The Sudanese grid before and after Merowe is modeled using a power system analysis software NEPLAN. Modeling of the Sudanese Grid is achieved by creating a single line diagram consisting of the interconnected Grid components. NEPLAN's user interface is used to enter the parameters that define each element in the system in consistency with the available data. NEPLAN's built-in analysis tools, including power flow, contingency, short circuit and stability analysis are used to simulate the performance of the Grid in different operating conditions. Simulation results are examined and discussed along with conclusions drawn from these results about Merowe's impact on grid performance.

1.5 Thesis Layout

Chapter Two discusses some aspects of power systems including design of selected power system elements and description of stability and control measures.

Chapter 3 presents the structure of the Grid before and after Merowe including a historical background, types of generation stations and their locations and capacities and the capability and topology of the transmission network.

Chapter 4 contains analysis of the performance of the Grid for both before and after Merowe cases. The analysis is preceded by an introduction to the analysis methods commonly used by power engineers to evaluate power network performance. The analysis performed includes load flow, contingency short circuit and stability studies. In Chapter 5, the analysis results are examined and a comparison between the before and after cases is presented. Conclusions are drawn about the impact of the Merowe project on the Grid and solutions to observed problems are proposed. The future of the Grid is then discussed in terms of load growth forecast and use of modern technology in enhancing network performance. The economic aspects of the proposed solutions are also briefly discussed. Detailed analysis results are presented in the appendix.

CHAPTER TWO
THE SUDAN NATIONAL GRID

2.1 Historical Background

Electric power generation in Sudan started in 1908 when the first D.C diesel generators were installed in Burri (east of Khartoum) with a capacity of 500 KW.

In 1925 Sudan government (under British Administration formed a company)(EL NOUR COMPNAY) to manage and develop the electric industry in Sudan and to meet the growth in demand in Khartoum. As a result, the generation units in Burri were replaced by larger ones with capacity of 3000 KW each.

In 1960 the Sudanese national government issued the law of Central Administration of Electricity and Water (CEWA) to work under supervision of the Ministry of Works, which expanded electricity services to the big cities of Sudan.

In 1962 the first hydroelectric power station was installed in Sennar dam with a capacity of 15 MW. It was followed in 1964 by Khasham Elgirba hydro power station (12.6 MW) and in 1971 by Roseires hydro power station (280 MW). In 2009 the installed 1250 MW generation capacity of Merowe dam power station followed.

Also in 1962 the first 110 KV transmission line was installed to transit power from Sennar to Khartoum followed in 1971 by the 220 KV transmission line between Roseires and Khartoum. In 1982 the authority to manage and develop electricity services was transferred to the newly formed National Electricity Corporation (NEC) and since then much development in generation and transmission networks has occurred.

2.2 Existing Power System

Recently a great development has occurred in generation and transmission systems of Sudan. In the following, we give a brief summary of generation plants, fuel resources and constraints existing

before Merowe as well as the structure of the transmission networks in both the National Grid and isolated areas.

2.3 National Grid Existing Generation Plants

In 2006 the total generation capacity available to the National Grid was approximately 800 MW of which about 60% is thermal power and 40% is hydro power distributed among the following power stations:

2.3.1 Thermal power stations:

1. Khartoum North Power Station

This station, located 4 km away from the Blue Nile river bank in Khartoum North, consists of 4-steam units fired on furnace (HFO-heavy fuel oil) and 4-gas turbine units fired on gas oil. The steam units 1 and 2 installed in 1984 are rated at 33 MW with available capacity of 30MW each while steam units 3 and 4, installed in 1993 are rated at 60MW with available capacity of 50MW each. Gas turbine units 1 and 2 were installed in 1992 and rated 20 MW with available capacity of 17 MW each. Gas turbines 3 and 4 were installed in 2001 and rated at 25 MW with available capacity of 20 MW each.

2. Garri1 Power Station

Garri1 power station was installed in 2003 in El Gaili, about 70 km north of Khartoum. It comprises combined cycle gas turbines (CCGT) with current available capacity of about 164 MW. Each of the two combined cycle modules is made by combining two 40 MW gas turbines with one 30 MW steam turbine.

3. Garri2 Power Station

Garri2 located in El Gaili near Garri1, is an open cycle gas turbines power station fired on gas oil. The power station houses three gas turbine units installed in 2003 with 40 MW rating and available capacity of 28 MW each. The current total available capacity of the station is about 84 MW.

2.3.2 Hydro Power Stations

1. Roseires Power Station

Roseiries hydro power station located on the Blue Nile river about 500 km south of Khartoum was the largest power plant in Sudan until the commissioning of Merowe plant. It consists of seven units with total installed capacity of 280 MW and total available capacity of 276.5 MW. These units were installed between 1971 and 1989.

2. Sennar power station

Sennar hydro power station is also located on the Blue Nile river about 300 km south of Khartoum. The station was installed in 1962 and consists of two units rated at 7.5 MW with current available capacity of 7 MW each.

3. Girba Power Station

Girba hydro power station located on Atbara River at Khasham El Girba town consists of:

- ✓ Two units each rated at 4.12 MW together with four 1900 hp electric motors which drive irrigation pumps.
- ✓ Three reversible axial flow pump turbines each rated at 2.07 MW in generating mode and 1.9 MW in the pumping mode.

All these units were installed between 1961 and 1963.

4. Jebel AuliaPower Station

Jebel Aulia power station is located on the White Nile river about 40 km south west of Khartoum. It consists of 80 hydro matrix turbines installed between 2003 and 2005 with total installed capacity of 28.8 MW.

2.4 Existing Transmission Networks

The Sudanese power network uses three transmission voltage levels, namely 220 KV, 110 KV and 66 KV, before Merowe while isolated area networks use distributed voltages of 33 KV and 11 KV.

The existing transmission system in Sudan (National Grid) comprises:

1. 220 KV double circuit line running about 500 km from Roseires substation in Blue Nile State to Khartoum State at KiloX substation via Sennar substation, Maringan substation, Hasahesa substation, Giad substation then crossing the Blue Nile river at KiloX substation into EidBabiker substation, to Garri substation and then to Shendi substation and Atbara substation (in River Nile State) about 300 km.
2. 110 KV line from Sennar substation to KiloX substation (in Khartoum) via Hag AbaAllaMaringan, Hasahesa, Giad and El Bagir substations. 110 kV line from Maringan substation to Gadaref substation via Fau substation.

   110 KV double circuit ring around Khartoum (about 70 km long) starting at KiloX S/S via Magirus, Ghaba, Omdurman, Mahadia, Ezergab, EidBabiker, Khartoum North and Kuku substations and then back to KiloX substation.

   110 KV double lines from KiloX substation to Faroug substation in the center of Khartoum.
3. 66 KV single line system in eastern state of Sudan from Girba to Kassala and from Girba to Gadaref where it is connected to the national grid via 110 kV line coming fromMaringan substation via Fau substation. All the 220 KV and some of the 110 kV substations were prepared with double busbar arrangement and step down transformers stepping the voltage down to 33 kV and 11 kV for local distribution systems.

The Grid described above is depicted in the following colour coded single line diagrams. The voltage levels at all bus-bars are indicated by the bus colour and the loading at each bus is shown in the accompanying table.

2.5 Sudan National Grid Load Curve

Like most power systems, the power system in Sudan follows a daily load cycle where the demand is highest during mid day and early evening (industrial, commercial and governmental) office air

conditioning & lighting and domestic loads are all on while night (people are sleep)and early morning demand is lowest.

Also the power system in Sudan follows weekly and annual cycles, where the load is lower during the weekend days than in the weekdays and lower during the cold season (winter) of the year than in the hot season (summer).

Like most power systems, the power system in Sudan follows a daily load cycle where the demand is highest during mid-day and early evening (industrial, commercial and governmental offices) air conditioning and lighting and domestic loads at the night (people are sleeping) and the demand is lowest in early morning .

Also the power system in Sudan follows weekly and annual cycles, where the load is lower during the weekend days than in the weekdays and lower during the cold season (winter) than in the hot season (summer) through the year

2011 Daily Load Curve

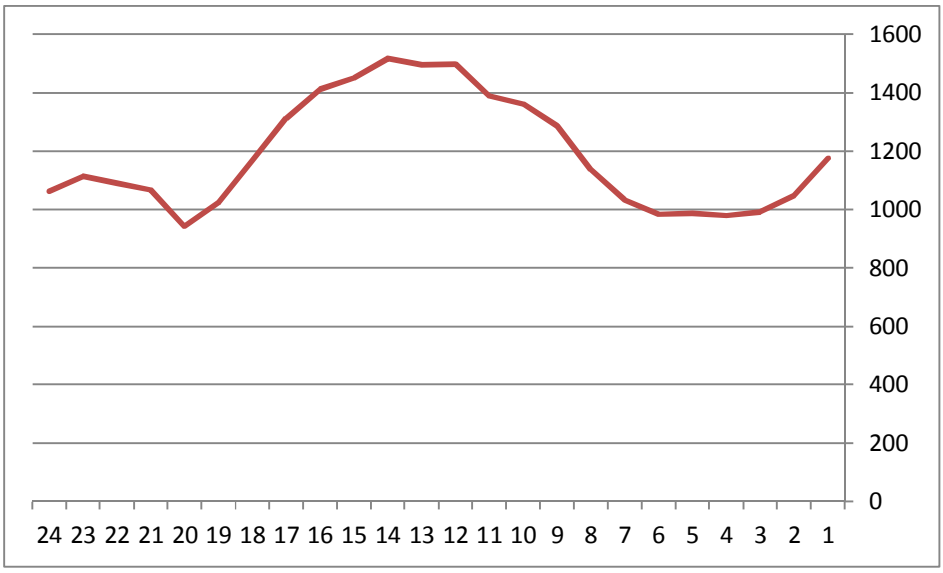

2011Daily Load Curve **Fig(2.1**

CHAPTER THREE
POWER SYSTEMS MODELLING

3.1 Introduction

The stability of an interconnected power system is its ability to return to normal or stable operation after having been subjected to some form of disturbance.[1] Conversely, instability means a condition denoting post disturbance loss of synchronism or falling out of step. Stability considerations have been recognized as essential part of power system planning for a long time. With interconnected systems continually growing in size and extending over vast geographical regions, it is becoming increasingly difficult to maintain synchronism between various parts of a power system.

Power system stability problems are classified into three basic types- steady state, dynamic and transient. The study of steady state stability is basically concerned with the determination of the upper limits of machine loadings before losing synchronism, provided the loading is increased gradually.

Dynamic instability is more probable than steady state instability. Small disturbances occur in a power system at all times (variations in loadings, changes in turbine speeds, etc.) and even though they are small enough not to cause the system to lose synchronism they do excite the system into a state of natural oscillations. The system is said to be dynamically stable if the oscillations amplitudes do not exceed a certain value and do not last beyond a small duration of time [2]. In other words, in a dynamically unstable system, oscillations amplitudes tend to be large and they persist for a long time. This kind of instability behaviour constitutes a severe threat to system security and creates very difficult operating conditions. Dynamic stability can be improved through the use of power system stabilizers. Effective dynamic system studies can only be carried out using computer programs, where simulations are run for 5-10 seconds and sometimes up to 30s. The

same simulation programs are, of course, applicable to transient stability studies.

Following a sudden disturbance in a power system, rotor speeds, rotor angular differences and power transfer undergo fast changes whose magnitudes are dependent upon the severity of disturbance. For a large disturbance, changes in angular differences may be large enough to cause the machines to fall out of step. This type of instability is known as transient instability and is a fast phenomenon usually occurring within 1 s for a generator close to the location of disturbance. There is a large range of disturbances that can occur in a power system that can lead to instability, the most significant of which are short circuits and the tripping of a large generator, a heavily loaded line or a large load.

The effect of short circuits (faults), the most severe type of disturbance to which a power system is subjected, must be determined in nearly all stability studies. During a fault, electrical power from nearby generators is reduced drastically, while power from remote generators is scarcely affected. In some cases, the system may be stable even with a sustained fault, whereas other systems will be stable only if the fault is cleared with sufficient rapidity. Whether the system is stable on occurrence of a fault depends not only on the system itself, but also on the type and location of fault, as well as the speed and method of fault clearing, i.e., whether cleared by the sequential opening of two or more breakers or by simultaneous opening and whether or not the faulted line is reclosed. The transient stability limit is almost always lower than its steady state counterpart but, unlike the latter, it may exhibit different values depending on the nature, location and magnitude of the disturbance.

Power systems today have many interconnected generating stations, each with multiple generation units and multiple loads. The machines located at any one point in a system normally act in unison. It is, therefore, common practice in stability studies to consider all the machines at one point as one large machine. Also machines which are

not separated by lines of high reactance are lumped together as one equivalent machine. Thus a multi-machine system can often be reduced to an equivalent few machine system. If synchronism is lost, the machines of each group stay together although they go out of step with other groups.

3.2 Dynamics of a Synchronous Machine

To understand the dynamics of a synchronous machine, the following definitions and derivations are presented.

The kinetic energy of the rotor at synchronous speed is

$$KE = \tfrac{1}{2} J \omega^2_{sm} \times 10^{-6} \text{ MJ} \qquad (3.1)$$

Where,

J = rotor moment of inertia in kg-m^2

ω_{sm} = synchronous speed in mechanical rad/s

But,

$\omega_s = (p/2)\omega_{sm}$ = synchronous speed in electrical rad/s

Where,

p = number of machine poles

Thus, $$KE = \tfrac{1}{2} J (2/p)^2 \omega^2_s \times 10^{-6} \text{ MJ} = \tfrac{1}{2} M\omega_s \qquad (3.2)$$

Where,

$M = J (2/p)^2 \omega_s \times 10^{-6}$ = moment of inertia in MJ-s/elect rad

Defining the inertia constant H as:

$$SH = KE = \tfrac{1}{2} M\omega_s \quad \text{MJ} \qquad (3.3)$$

Where, S = machine rating (base) in MVA (3-phase)

H = *inertia constant* in MJ/MVA or MW-s/MVA,

it immediately follows that

$$M = 2SH/\omega_s = SH/\pi f \quad \text{MJ-s/elect rad.} \qquad (3.4)$$

Taking S as base, M in per unit is

$$M\,(p.u.) = H/\pi f \quad \text{s}^2\text{/elect rad.} \qquad (3.5)$$

$= H/180f$ s^2/elect deg.

The inertia constant H has a characteristic value or a range of values for each class of machines. The table (3.1) below lists some typical inertia constants.

Table (3.1) Machines Inertia Constant (H)

Type of Machine	Inertia Constant H Stored Energy in MW sec per MVA
Turbine Generator Condensing 1800 rpm	9 – 6
Condensing 3000 rpm	7 – 4
Non Condensing 3000 rpm	4 – 3
Waterwheel Generator Slow speed < 200 rpm	2 – 3
High speed > 200 rpm	2 – 4
Synchronous Condenser Large Small	 1.25 1.00
Synchronous motor with loads varying from 1.0 to 5.0 p.u	2.00

3.3 The Swing Equation

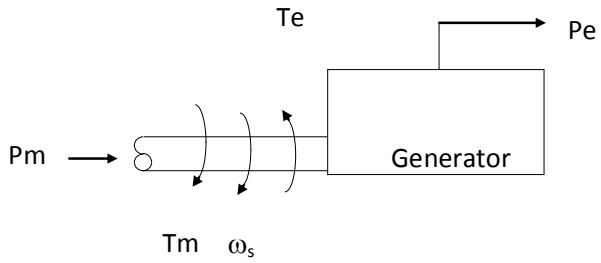

Figure (3.1) Synchronous machine Torque, Speed and power flow

The figure (3.1). above shows the torque, speed and flow of mechanical and electrical powers in a synchronous machine. It is assumed that the windage, friction and iron-losses are negligible. The differential equation governing the rotor dynamics can then be written as [3]

$$J\frac{d^2\theta_m}{dt^2} = T_m - T_e \quad \text{Nm} \tag{3.6}$$

Where

θ_m= rotor angle in mechanical radians

Tm= turbine torque in Nm;

Te = electromagnetic torque developed in Nm. Both torques above assume negative values for a motoring machine.

While the rotor dynamics shown by the equation above take place, rotor speed changes by an insignificant magnitude for the time period of interest (1s). The equation can therefore be converted into its more convenient power form by assuming the rotor speed to remain constant at synchronous speed ω_{sm}. Multiplying both sides of the equation by ω_{sm}

$$J\omega_{sm}\frac{d^2\theta_m}{dt^2} = P_m - P_e \tag{3.7}$$

Where,
Pm = mechanical power
Pe = electrical power output; (stator copper losses neglected)
Dividing the above equation by *p/2*to convert both ω_{sm} and $\theta_m$to electrical units and defining electrical and mechanical power in MWs by dividing by 10^{-6},yields

$$J\left(\frac{2}{p}\right)^2 \omega_s \times 10^{-6} \frac{d^2\theta_e}{dt^2} = P_m - P_e \quad \text{MW} \tag{3.8}$$

Or

$$M\frac{d^2\theta_e}{dt^2} = P_m - P_e \text{MW} \tag{3.9}$$

Where,
θ_e = rotor angle in electrical radians
It is more convenient to measure the angular position of the rotor with respect to a synchronously rotating reference. Let
$\delta = \theta_e - \omega_s t$; rotor angular displacement from synchronously rotating reference (called torque angle or power angle)
Taking derivatives

$$\frac{d^2\theta_e}{dt^2} = \frac{d^2\delta}{dt^2} \tag{3.10}$$

Hence,

$$M\frac{d^2\delta}{dt^2} = P_m - P_e \quad \text{MW} \tag{3.11}$$

With M defined in terms of inertia constant H of the machine

$$\frac{SH}{\pi f}\frac{d^2\delta}{dt^2} = P_m - P_e \quad \text{MW} \tag{3.12}$$

Dividing throughout by S, the MVA rating of the machine,

$$\frac{H}{\pi f}\frac{d^2\delta}{dt^2} = P_m - P_e \quad \text{p.u.} \tag{3.13}$$

This non-linear second order differential equation is called the swing equation and it describes the rotor dynamics for a synchronous machine (generator/motor). The damping dδ/dt term is absent because of the assumption of a lossless machine and neglecting the torque of the damper winding. This assumption leads to pessimistic results in transient stability studies –since damping helps to stabilize the system. Damping, which is a function sinδ must of course be considered in a dynamic stability study.

3.4 Multi-machine System

In a multi-machine system a common system base must be chosen. Let

S_{mach} = machine rating (base)

S_{system} = system base

Then,

$$\frac{S_{mach}}{S_{system}}\left(\frac{H_{mach}}{\pi f}\frac{d^2\delta}{dt^2}\right) = \left(P_m - P_e\right)\frac{S_{mach}}{S_{system}} \tag{3.14}$$

Or,

$$\frac{H_{system}}{\pi f}\frac{d^2\delta}{dt^2} = P_m - P_e \text{ p.u. on system base} \tag{3.15}$$

Where,

$$H_{system} = H_{mach}\left(\frac{S_{mach}}{S_{system}}\right) = \text{machine inertia constant on system base.} \tag{3.16}$$

3.5 Machines Swinging Coherently

Consider the swing equations of two machines on a common system base.

$$\frac{H_1}{\pi f}\frac{d^2\delta_1}{dt^2} = P_{m1} - P_{e1} \tag{3.17}$$

$$\frac{H_2}{\pi f}\frac{d^2\delta_2}{dt^2} = P_{m2} - P_{e2} \tag{3.18}$$

Since the machines swing together (coherently or in unison)

$\delta_1 = \delta_2 = \delta$

Adding the two equations together

$$\frac{Heq}{\pi f}\frac{d^2\delta}{dt^2} = P_m - P_e \qquad (3.19)$$

Where,

$P_m = P_{m1} + P_{m2}$, $P_e = P_{e1} + P_{e2}$ and $H_{eq} = H_1 + H_2$

The two machines swinging coherently are thus reduced to a single machine. The equivalent inertia can be written as.

$$H_{eq}=H_{1mach}\, S_{1mach}/S_{system} + H_{2mach}\, S_{2mach}/S_{system} \qquad (3.20)$$

The above results are easily extendable to any number of machines swinging coherently.

3.6 Simplified Machine Model

For a non-salient pole machine, the per phase induced emf-terminal voltage under steady state conditions is

$$E = V + jX_dI_d + jX_qI_q;\ X_d<X_q \qquad (3.21)$$

Where, $I = I_d + I_q$

Under transient conditions $X_d \rightarrow X'_d<X_q$ But,

$X_q = X'_q$since the main field is on the direct axis

$X'_d<X_q$; but the difference is small

The voltage equation during transient conditions are then,

$$E = V + j\,X'_d\,I_d + j\,X'_q\,I_q = V + j\,X_q(I - I_d) + j\,X'_d\,I_d \qquad (3.22)$$

$$= (V + j\,X_qI) + j(X'_d - X_q)I_d$$

The phasor diagram corresponding to the above equation is shown belowin Figure 3.2

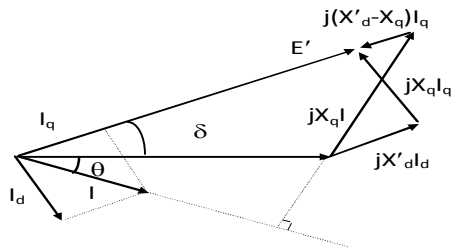

Figure (3.2) phasor diagram of voltage equation during transient conditions

Since under transient conditions, $X'_d < X_q$ but X_q remains almost unaffected, it is fairly valid to assume that

$$E' = V + j\,X_q I = V + j\,X'_d\,I \qquad (3.23)$$

The machine model corresponding to the equations above is shown below in Figure (3.3)

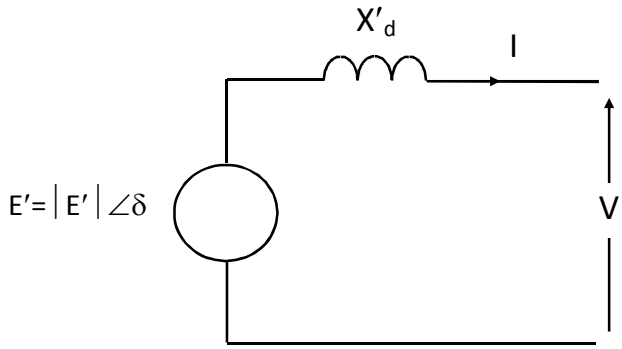

Figure (3.3) Electrical Machine Model(under transient condition

3.7 Power Angle Curve for a Two Machine System

Consider a transient stability study for a system of two machines. Because the emf behind transient reactance of each generator E′ remains constant throughout the study while the terminal voltage V is allowed to vary, the nodes

of the stability network will pertain to E′ rather than V, in contrast to load flow studies. All other busbars in the system will be eliminated using a node elimination technique. We will end up with only two busbars separated by a transfer reactance.

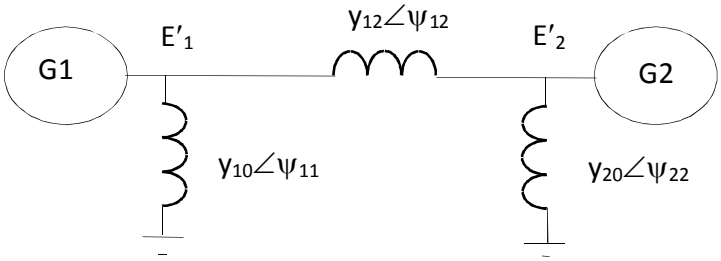

Figure (3.4) Two Machines elimination node

$\mathbf{Y_{bus}}$ for this reduced network is

$$\begin{vmatrix} Y11 & Y12 \\ Y21 & Y22 \end{vmatrix}$$

Complex electrical power injected into node 1 is given as

$$\mathbf{E'_1 I^*_1} = P_1 + j\,Q_1$$

$$= \mathbf{E'_1(Y_{11}E'_1)^*} + \mathbf{E'_1(Y_{12}E'_2)^*} \qquad (3.24)$$

Since in the solution of the swing equation only real power is involved

$$P_1 = E'^2_1 G_{11} + E'_1\, E'_2 Y_{12}\cos(\delta_1 - \delta_2 - \psi_{12}) \qquad (3.25)$$

If the system is lossless, then all G's will be = 0; hence

$$P_1 = E'_1\, E'_2 Y_{12}\cos(\delta_1 - \delta_2 - 90)$$

$$= E'_1\, E'_2 B_{12}\sin(\delta_1 - \delta_2) \qquad (3.26)$$

This is the well known power angle equation for a two machine system. The electrical power for the second generator is written as

$$P_2 = E'_1\, E'_2 B_{21}\sin(\delta_2 - \delta_1) \qquad (3.27)$$

The swing equations for the two machines are then:

$$\frac{H_1}{\pi f}\frac{d^2\delta_1}{dt^2} = P_{m1} - P_{e1} \qquad (3.28)$$

$$\frac{H_2}{\pi f}\frac{d^2\delta_2}{dt^2} = P_{m2} - P_{e2} \tag{3.29}$$

Respectively.

3.8 Two-Machine to One-Machine-Infinite-Busbar System

We have discussed the case of a system reduced to two machines separated by transfer admittance. This system can be further simplified by converting it to a one-machine-infinite-busbar system. Under steady state conditions a balance exists between the mechanical and electrical power in each machine. Assume that under transient conditions a net power transfer equal to Pmech - Pe = ΔP flows from the first machine to the second. The second machine will be motoring iePmech - Pe = -ΔP. The relative load angle between the two machines is δ = δ1 - δ2.

The swing equation for the first machine is

$$\frac{d^2\delta_1}{dt^2} = \frac{\pi f}{H_1}\Delta P \tag{3.30}$$

and, for second machine

$$\frac{d^2\delta_2}{dt^2} = -\frac{\pi f}{H2}\Delta P \tag{3.31}$$

subtracting the two equations,

$$\frac{d^2\delta}{dt^2} = \left(\frac{\pi f}{H1} + \frac{\pi f}{H2}\right)\Delta P \tag{3.32}$$

The equivalent inertia constant for the resulting one machine is thus

$1/H_{eq} = 1/H_1 + 1/H_2$; thus (3.33)

$H_{eq} = H_1 \cdot H_2 /(H_1 + H_2)$ (3.34)

3.9 Transient Stability Analysis

In contrast to small disturbance stability, there are no generalized criteria available for determining system stability with large disturbances (transient stability). The practical approach is to list,

according to experience and sound engineering judgment, all perceivable important severe disturbances along with possible locations. Numerical solution of the swing equation (or equations for a multi-machine case) is then obtained in the presence of such disturbances giving a plot of δ vs. t called the swing curve. If δ starts to decrease after reaching a maximum value, it is normally assumed that the system is stable and the oscillation of δ around the equilibrium point will decay and finally die out. As already pointed out in the introduction, important severe disturbances are a short circuit or a sudden loss of load.

Some of the assumptions that are put forward to simplify the transient stability analysis are listed below.

1. Damping term contributed by the synchronous machine damper windings and losses in rotor iron is ignored. This leads to a pessimistic result for the transient stability limit.
2. Rotor speed is assumed to be synchronous. In fact it varies insignificantly during the period of the study.
3. Mechanical input to the machine is assumed to remain constant during the transient, i.e., regulating action of the governor-turbine is ignored. This also leads to pessimistic results.
4. Voltage behind transient reactance (E'_q) is assumed to remain constant. Actions of flux decay and AVR are neglected. The role of the AVR is usually in the direction of aiding transient stability, and thus neglecting it leads to pessimistic study results.
5. Loads are modeled as constant admittances. This is a reasonably accurate representation.

The steps carried out for a single-machine-infinite-busbar system transient stability study are listed below:

1. From prefault loading, determine the voltage behind transient reactance and the load angle δ_0 of the machine with reference to the infinite bus.

2. For the specified fault, determine transfer admittance during the fault and hence form the swing equation during fault.
3. Starting with $\delta = \delta_0$, solve the swing equation using a numerical technique to obtain δ as a function of time t.
4. After clearance of fault at a time t_c , form the *post-fault* swing equations from the post-fault transfer admittances and continue calculation of δ as a function of time t up to, say, 1 second.
5. If δ goes through a maximum and starts to reduce, the system is considered stable. But if it continues to increase indefinitely, the system is transiently unstable.

The critical clearing time, after which clearing the fault would lead to instability can be assessed by repeating the above study, starting with a small value of tc then increasing it in small steps, until unstable behavior is observed.

Alternatively a much more elegant technique called the equal area criterion maybe used.

3.10 Equal Area Criterion

Consider the swing equation for a one-machine-infinite busbar system.

$$\frac{d^2\delta}{dt^2} = \frac{1}{M}\left(P_{mech} - P_e\right) = \frac{P_a}{M} \quad ;P_a \text{ is the accelerating power} \qquad (3.35)$$

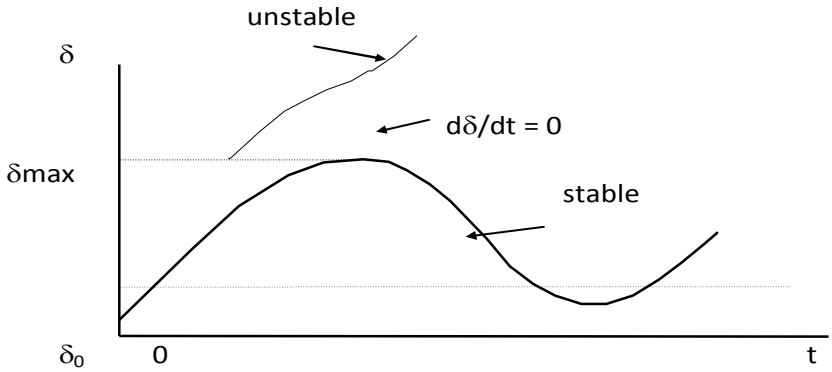

Figure (3.5) Single Machine Busbar system stability condition

If the system is unstable δ increases indefinitely and the machine loses synchronism. On the other hand if the system is stable δ will go through maximum at which
dδ/dt = 0. This condition can be stated as a stability criterion for this particular case.
The machine will be considered unstable if dδ/dt> 0 for a sufficiently long time (1 second).
Multiplying both sides of the swing equation by 2dδ/dt yields,

$$2\frac{d\delta}{dt}\frac{d^2\delta}{dt^2} = 2\frac{P_a}{M}\frac{d\delta}{dt} \tag{3.36}$$

Integrating with respect to *t*

$$\left(\frac{d\delta}{dt}\right)^2 = \frac{2}{M}\int_{\delta_0}^{\delta} P_a d\delta \tag{3.37}$$

$$\frac{d\delta}{dt} = \left(\frac{2}{M}\int_{\delta_0}^{\delta} P_a d\delta\right)^{\frac{1}{2}} \tag{3.38}$$

Where, δ_0 is the initial rotor angle. The condition for stability is dδ/dt = 0. Hence,

$$\int_{\delta_0}^{\delta} P_a d\delta = 0 \qquad (3.39)$$

The condition of stability can therefore be stated as: **the system is stable if the area under P_a in the power angle curve reduces to zero at some value of δ.** In other words, the positive (accelerating) area must be equal to the negative (decelerating) area. This is the Equal Area Criterion.

Two disturbance types will be used to illustrate the equal area criterion:

(a)Sudden Change in Mechanical Input

Consider a single machine feeding an infinite busbar through a transmission link as below.

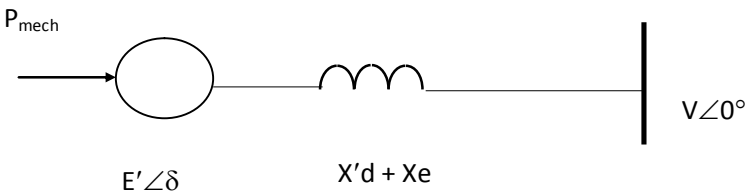

Figure (3.6) Single Machine feeding an infinite Bus bar

Under steady state operation

$$P_{mech} = P_m \sin\delta_0 \qquad (3.40)$$

This is indicated by the point a in the power angle diagram shown below. [3]

Let the mechanical input to the rotor be suddenly increased to Pm1 (by opening the steam valve). The accelerating power causes the rotor speed ω and the rotor angle δ to increase. Pa is positive (accelerating) as shown by the shaded area A1.

At point **b**,P_{m1} - P_e = 0, hence P_a = 0 , but the rotor angle continues to increase as $\omega > \omega_s$. P_a now becomes negative (decelerating) as shown in shaded area A_2. At point **c**$\omega = \omega_s$ie $d\delta/dt = 0$. Hence according to our criteria, $A_1 = A_2$.

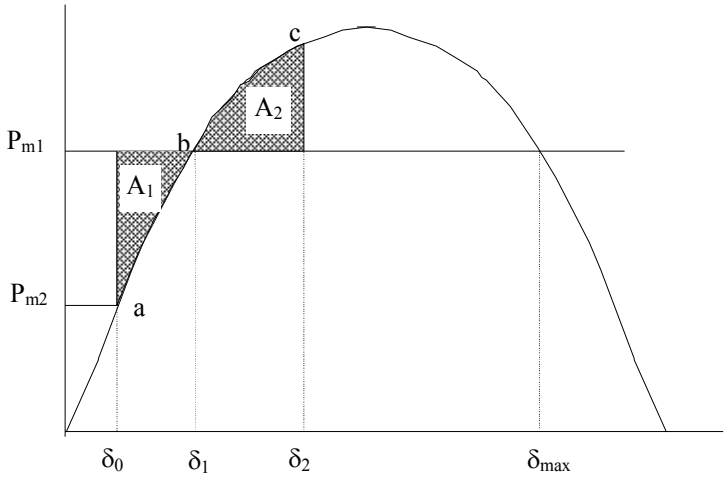

Figure (3.7) power angle diagram stability condition

$$A_1 = \int_{\delta_0}^{\delta_1} (P_{m1} - P_e) d\delta \tag{3.41}$$

$$A_2 = \int_{\delta_1}^{\delta_2} (P_e - P_{m1}) d\delta \tag{3.42}$$

For the system to be stable, it should be possible to find an angle δ2 such that A1 =A2. The maximum possible value for δ2 is obtained as δmax (see figure) $\delta_{max} = \pi - \delta_1$ (3.43)

Any further increase in Pm1 means the area A2. is less than area A1 , leading to an unstable situation.

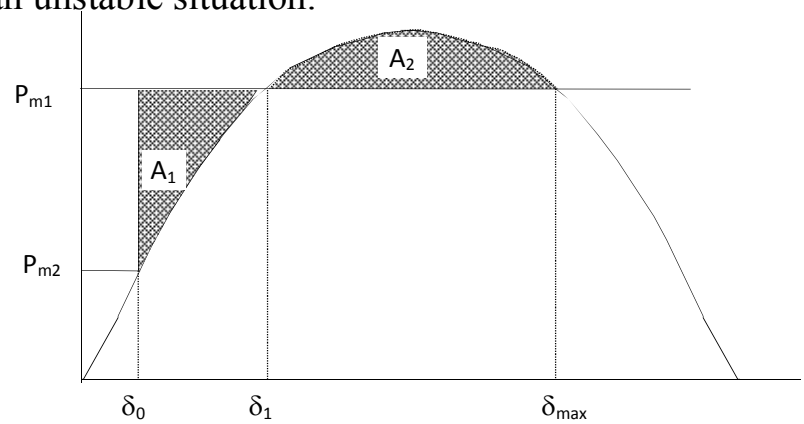

Figure (3.8) power angle diagram instability condition

(b) Short Circuit on One of Parallel lines

Consider a single machine tied to an infinite bus through two parallel lines as shown in figure below. Let us assume that a three phase short circuit occurs at the generator end of line 2.

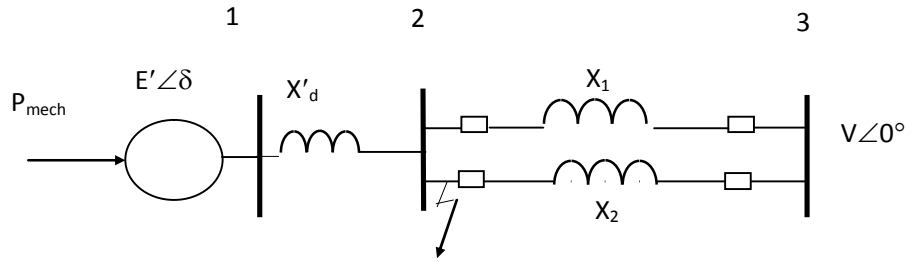

Figure (3.9) Three phase short circuit condition

Before the fault the total transfer reactance between bus 1 and 3 is X′d + X1//X2

To simulate a three phase fault at bus 2 we connect it to the reference. The transfer reactance between generator and infinite bus now becomes infinite. Hence no power can be transferred during fault conditions.

If the fault is cleared by removing line 2 the post-fault transfer reactance is now found as X′d+ X1.

The transfer reactance in this case increases over the prefault value.[2]

Plots of the power angle curves for the three cases are shown below

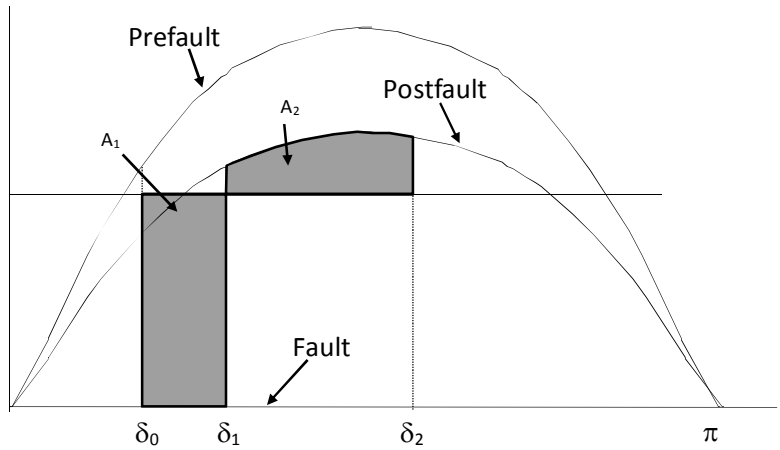

Figure (3.10) power angle curves of prefault, fault and postfault

It is not necessary that the transfer power during a fault becomes zero. The above example represents an extreme case. Normally there will a value of transfer reactance although large, during fault conditions. This can be demonstrated if the above fault was assumed to occur in the middle of line 2 as shown in example below. It is not common however, in computer applications of transient stability studies to implement a fault in the middle of lines, since this requires introducing new busbars. Faults are normally assumed to occur at busbars. This also covers, without much loss of accuracy faults within the neighborhood of line ends.

Critical Clearing Time: It is usually desired for purposes of protection settings, to find the critical clearing time instead of the critical clearing angle. If the trajectory of angle against time were known, this value would simply be the time instant corresponding to δCR. The swing equation for a one-machine-infinite-busbar system is

$$\frac{d^2\delta}{dt^2} = \frac{\pi f}{H}(P_{mech} - P_m \sin\delta) \qquad (3.44)$$

This equation must be solved to determine the angle δ as a function of time t. It is not possible, however to carry out direct integration to solve

the problem; rather step-by-step numerical methods are needed to plot δ. To simplify, we break down the differential equation into two differential equation of first order derivatives.

$$\frac{d\omega}{dt} = \frac{\pi f}{H}(P_{mech} - P_m \sin\delta) \tag{3.45}$$

$$\frac{d\delta}{dt} = \omega - \omega_s \tag{3.46}$$

The initial conditions are at $t = 0$, $\delta = \delta_0$ and $\omega = \omega_S$

One possible numerical method of solution is the Runge-Kutta algorithm. Another method is the modified Euler algorithm. Alternatively mathematical packages such as MATLAB may be used. Usually a number of plots are generated for different clearing times and the behavior of the resulting curves examined to determine stability. The example below illustrates a one machine-infinite-busbar case.[4]

3.11 Power System Control

Power system control is the duty of maintaining certain conditions pertaining to the quality, reliability and economy of the power system operation. These conditions include supplying the demand reliably at minimum possible cost and with adequate reserve [5]. Quality characteristics are constant frequency, bus voltage levels that are close or equal to respective ratings and reliability of supply. To meet these conditions control devices and schemes are applied. Control devices such as prime mover and excitation controllers are applied at the generator level, while transformer tap changers and reactive compensation devices are applied at the transmission system level. All of these control elements work together to maintain steady state operation conditions during normal operation and to bring the system back to normalcy after a disturbance. Good system design and proper protection and prevention schemes play important roles in power system control.

Below, some of the control elements that are typically applied in power system applications are presented.

3.11.1 DC Excitation System

Shown below in Figure (3.11) is a simplified schematic diagram of a typical dc excitation system with an amplidyn voltage regulator and the model of an IEEE typeDC1Aexcitation system.[6]

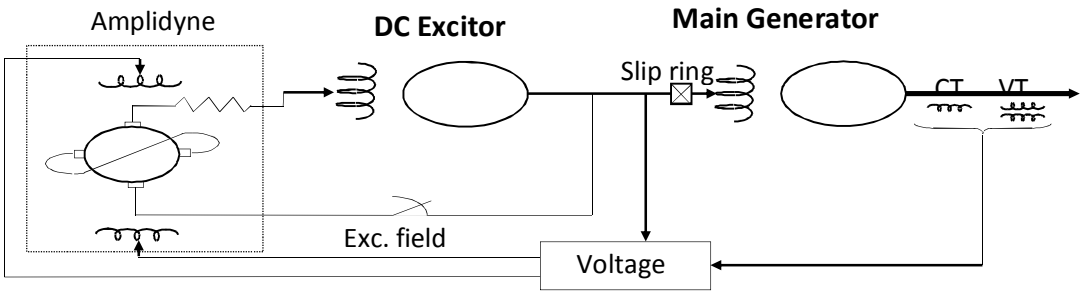

Figure (3.11) Simplified DC Excitation System with amplidyn voltage regulator

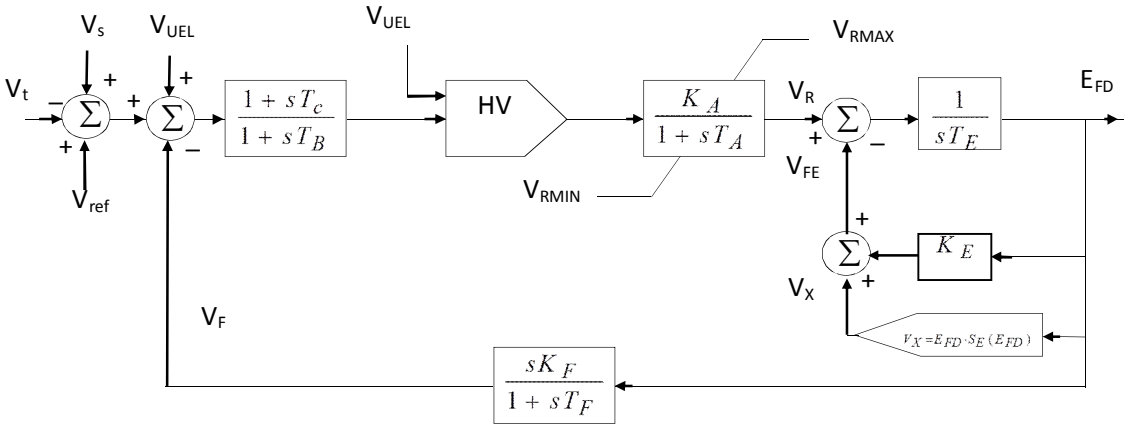

Figure (3.12) Control block diagram of DC exciter

Where,

Vt is machine terminal voltage, which is denoted by Vcin case a load compensation circuit is used meaning that Vc is the output from the load compensating circuit.

Vs, the output from a power system stabilizer takes a 0 value under steady state conditions while V ref takes a value that depends on the power system loading conditions so that the error signal results in the required field voltage Efd.

TC and TB represent lag and lead compensation respectively.

KA and TA are the amplifier gain and time constant respectively.
UEL, the under excitation limiter by way of a High Value gate determines and passes only the higher value of its two inputs.
KF and TF are the stabilizing loop gain and time constant. The stabilizing loop is necessary because the excitation system contains elements with significant time delays. Unless a very low steady state regulator gain is used, the excitation control is unstable when the generator is on open circuit. Thus derivative feedback is used to improve the dynamic response of the control system. It is usually realized by a series transformer as shown below.

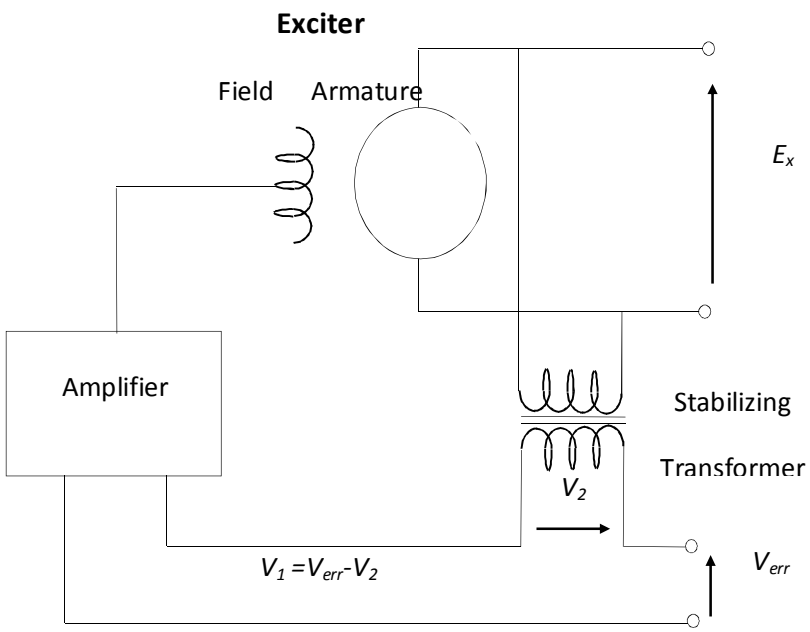

Figure (3.13) Excited Circuit with Stabilizing Transformer

3.11.2 The DC Exciter Model

The exciter is modeled as shown below in Figure (3.14)

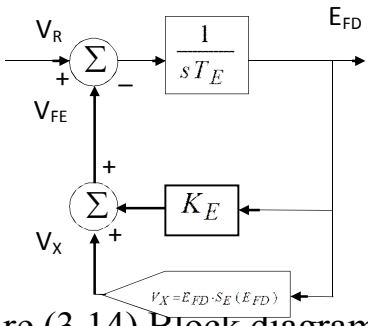

Figure (3.14) Block diagram of DC Exciter

The function $S_E(E_{FD})$ accounts for saturation of the exciter and depends on the value E_{FD}.

At steady state the following summation

$$V_R - E_{FD}K_E - E_{FD}S_E(E_{FD}) = 0 \qquad (3.47)$$

It is evident that the function $S_E(E_{FD})$ accounts for the non linear relation between voltage regulator input to excitor, V_R, and excitor output voltage E_{FD}. A commonly used function for $S_E(E_{FD})$ is $A_{EX}e^{B_{EX}E_{FD}}$. For a self excited exciter the value of K_E is initially computed such that $V_R = 0$.

3.11.3 AC Excitation Systems

The excitation systems of this category utilize alternators (ac machines) as sources of the main generator excitation power. Usually, the excitor is on the same shaft as the turbine generator. The ac output of the excitor is rectified by either controlled or non-controlled rectifiers to produce the direct current needed for the generator field. The rectifiers may be stationary or rotating. The following figure illustrates a field controlled alternator rectifier system.

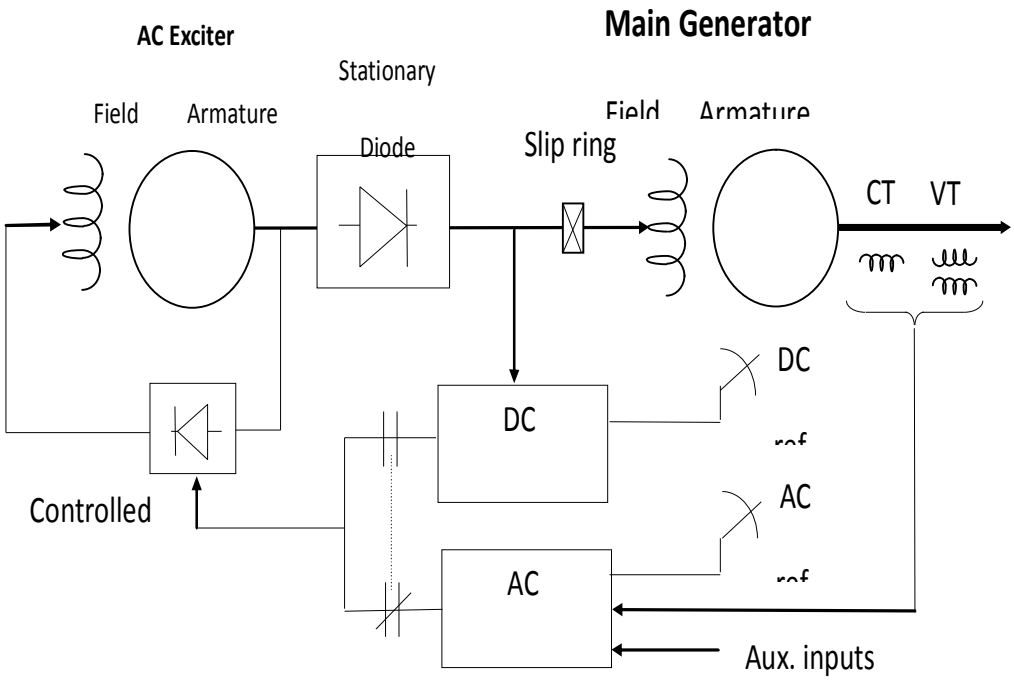

Figure (3.15) Field controlled alternator rectifier excitation system

The second system shown below in figure (3.16) , illustrates an alternator supplied controlled rectifier system.

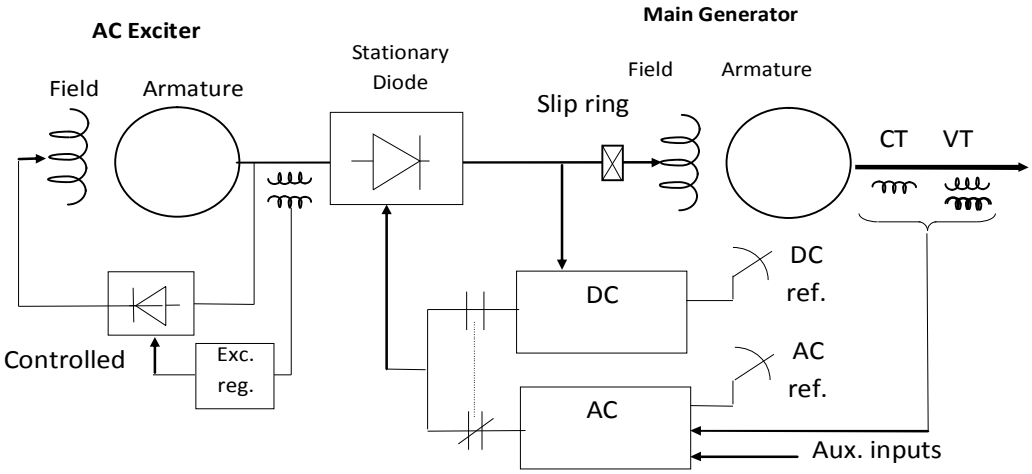

Figure (3.16) Alternator supplied controlled – rectifier excitation system

The third AC system shows a typical brushless excitation system figure (3.17).

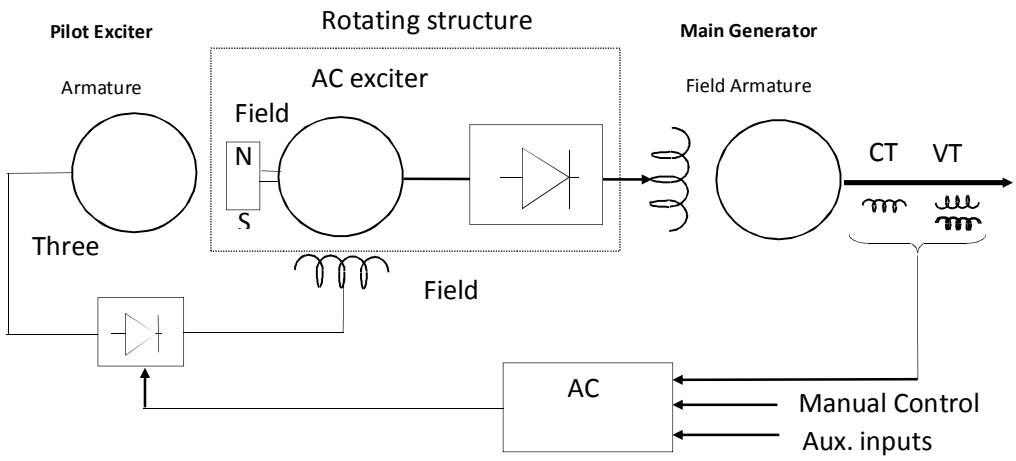

Figure (3.17) Brushless excitation system

3.11.4 AC Exciter Model

The exciter model is similar to that of the DC exciter as shown below in figure (3.18) except that the exciter voltage VE is represented by the no load voltage as determined by the saturation function SE. The main generator field current IFD represents the exciter load current, and the negative feedback of KDIFD accounts for the armature reaction demagnetizing effect.

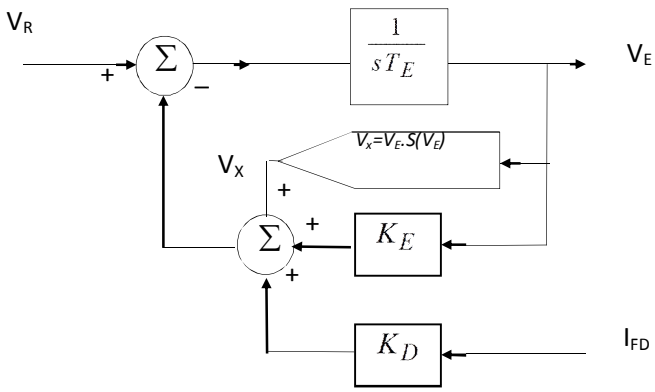

Figure (3.18) Block diagram of an AC Exciter

3.11.5 Static Excitation Systems

All components in these systems are stationary. Controlled or uncontrolled static rectifiers supply the excitation system directly to the field of the main synchronous generator through slip rings. The supply of power to the rectifiers is from the main generator (or the station auxiliary bus) through a transformer to step down the voltage to an appropriate level, or in some cases from auxiliary windings in the generator.

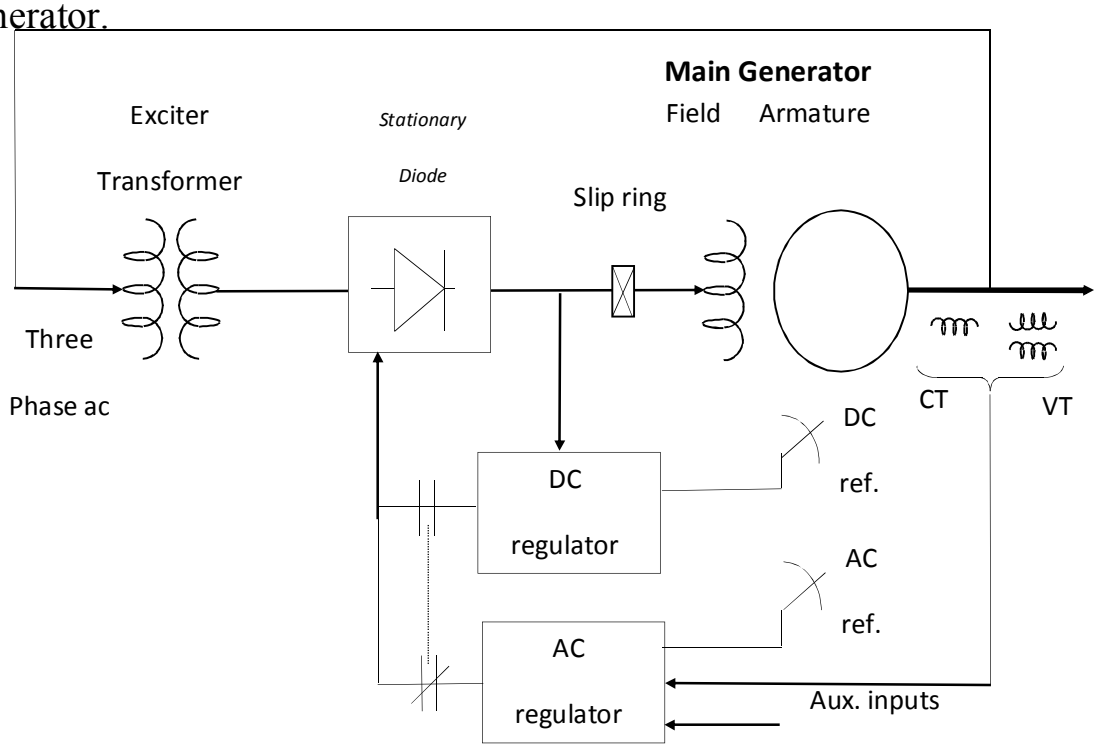

Figure (3.19) Control rectifier excitation system

3.12 Dynamic Performance Measures

Since the system is non-linear, it is convenient to classify the dynamic performance into large signal performance, where the non-linearity is important and small-signal performance, where the response is linear.

3.12.1 Large Signal Performance Measures

- Excitation system ceiling voltage: maximum direct voltage that the excitation system is able to supply under specified conditions.
- Excitation system ceiling current: Maximum direct current that the excitation system is able to supply for a specified time.
- Excitation system voltage time response: the excitation system output voltage as a function in time under specified conditions.
- Excitation system voltage response time: the time in seconds for the excitation to attain 95% of the difference between ceiling voltage and rated load field voltage under specified conditions.
- High initial-response excitation systems: An excitation system having a voltage response time of 0.1 seconds or less. It represents a fast acting system.
- Excitation system nominal response: The rate of increase of the excitation system determined from the excitation system voltage response curve, divided by the rated field voltage.

3.12.2 Small Signal Performance Measures

Small signal performance can be measured by either a time response or a frequency response to change in input. The typical time response of a feedback control system to a step change in input is shown below in figure (3.20).

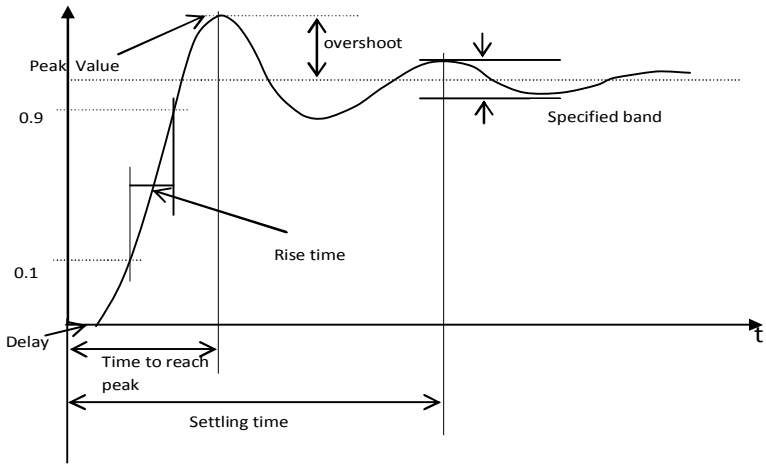

Figure (3.20) Small Signal Performance Measures by time and frequency

An open-loop frequency response characteristic of an excitation control system with generator open-circuited is shown below in figure (3.21).

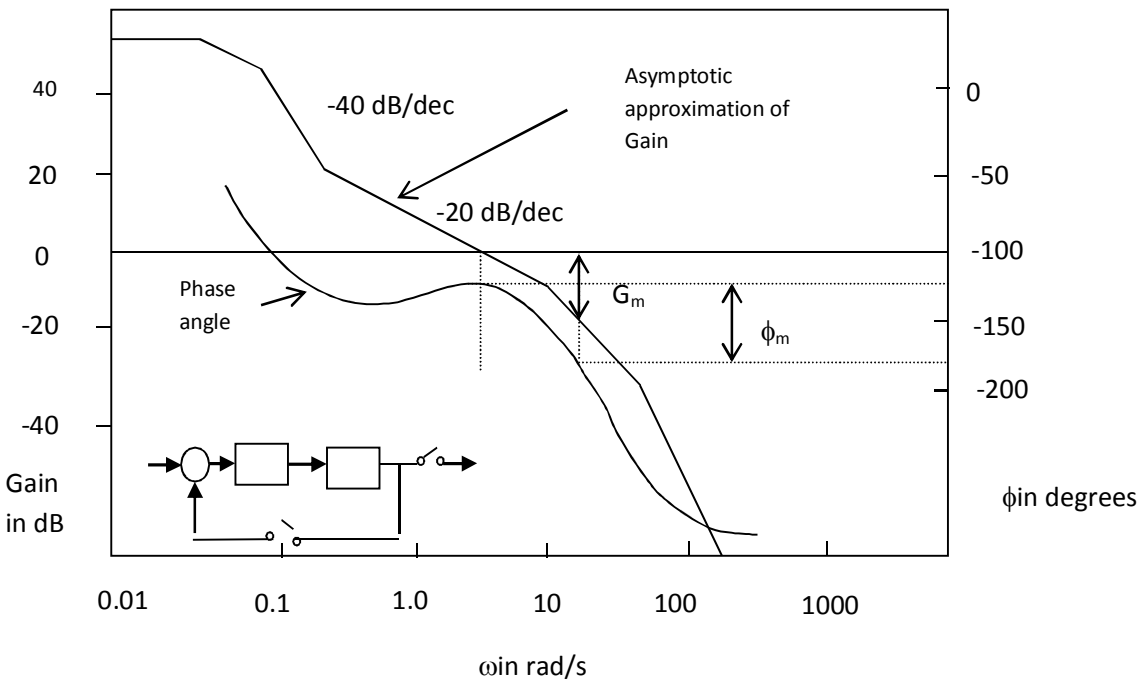

Figure (3.21)An Open loop Frequency response characteristic of an excitation control system

The performance indices associated with the open loop frequency response are the low frequency gain G, cross-over frequency ωC, phase margin ϕm , and gain margin Gm . Larger values of G provide better steady-state regulation, and larger cross-over frequency, ωC, indicate faster response. Larger values of phase margin ϕm and gain margin Gm provide a more stable excitation control loop.

In tuning the voltage regulator, an improvement to one index will likely result in the detriment of other indices. For example, an increase in regulator gain will shift the gain curve upwards. This has the beneficial effect of increasing the low-frequency gain and cross-over frequency, but has the undesirable effect of decreasing the gain margin and phase margins. In general a choice of a phase margin of 40° or more, and a gain margin of 6 dB or more is considered to be good design practice for obtaining a stable, non-oscillatory voltage regulation system.

The Figure (3.22) below shows the corresponding closed-loop frequency response with the generator open-circuited.

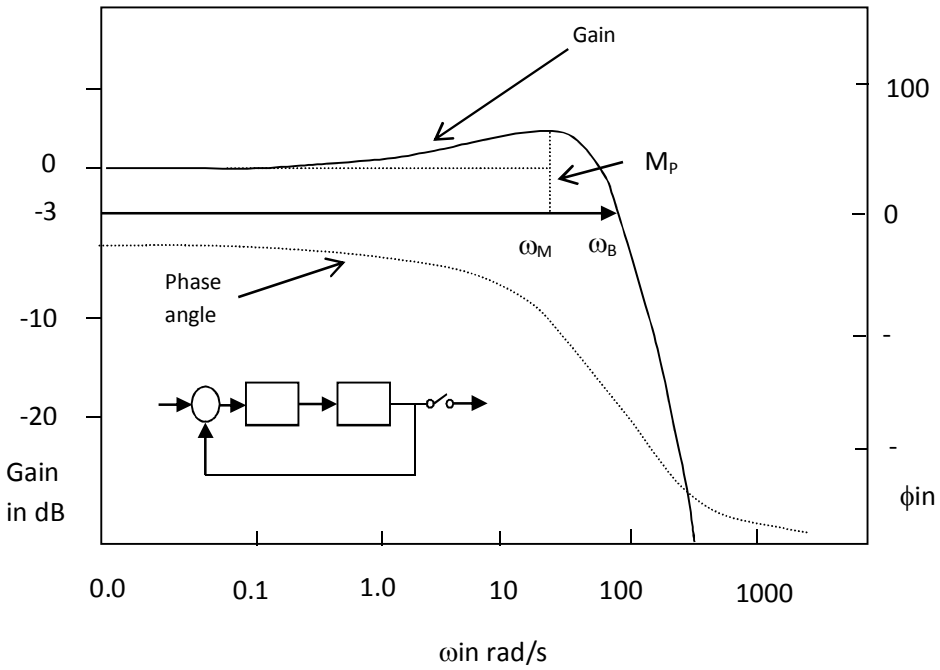

Figure (3.22). Closed-loop frequency response with the generator open-circuited.

The indices of interest associated with closed-loop frequency response are the bandwidth ωB and peak value MP.

A high value of MP (>1.6) is indicative of an oscillatory system exhibiting large overshoot in its transient response. In general, it is considered good practice to choose a value between 1.1 and 1.5. Bandwidth is an important closed-loop frequency response index. Larger values indicate faster response. It approximately describes filtering or noise rejection characteristics of the system.

The performance indices given above are applicable to a generator on open circuit or feeding an isolated load. If, however the generator is connected to a power system the control system becomes a multi-loop, multi-variable, high order control system. For such a system the performance indices described above are not applicable. Instead, state space methods using eigenvalue techniques are used to assess stability.

3.13 Governor-Turbine System

The prime sources of electrical energy supplied by the utilities are the kinetic energy of water and the thermal energy derived from fossil fuel and nuclear fission. The prime movers convert these sources of energy into mechanical energy that is, in turn, converted to electrical energy by synchronous generators. The prime mover governing systems control power and frequency. This is usually referred to as load-frequency control or automatic generation control (AGC). The basic function blocks are shown below in figure (3.23).

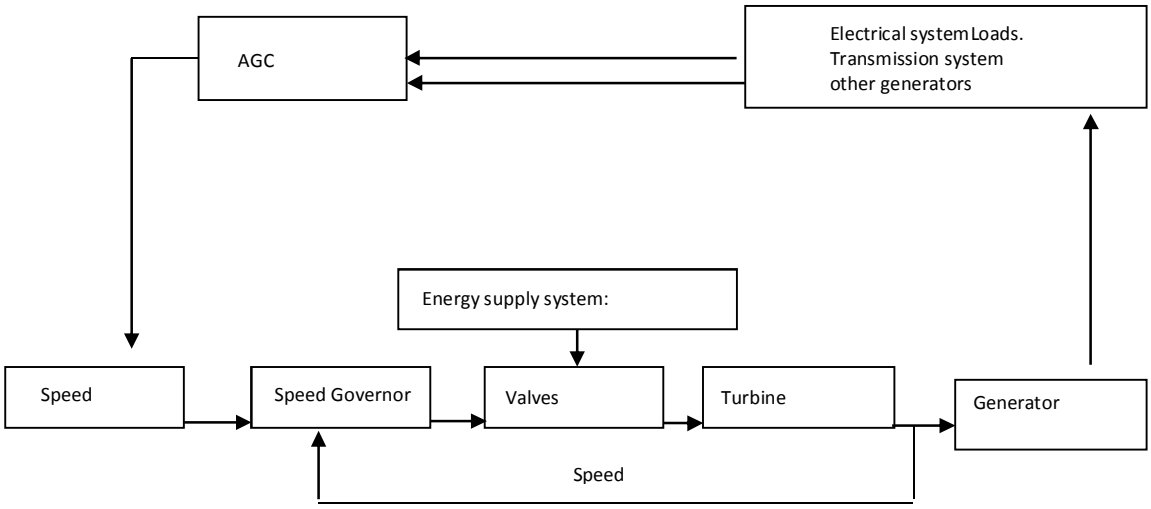

Figure (3.23) The (AGC) basic function blocks

3.13.1 Hydraulic Turbines

Two types of turbines are used, Impulse Turbine and Reaction Turbine. The impulse type is also known as the Pelton Turbine and is used for high water heads of 300m or more.

The reaction type is used for medium heads (45 - 300 m,Francis Turbine), and low heads (up to 45 m, Kaplan Turbine).

In an attempt to model the hydraulic turbine we shall assume that.

1. The hydraulic resistance is negligible.
2. The penstock pipe is inelastic and the water is incompressible.
3. The velocity of the water varies directly with the gate opening and with the square root of the net head.
4. The turbine output power is proportional to the product of head and volume flow.

The Turbine and penstock characteristics are determined by three basic equations relating to the following:

- Velocity of water in the penstock, U.
- Turbine mechanical power, P_m.
- Acceleration of water column.

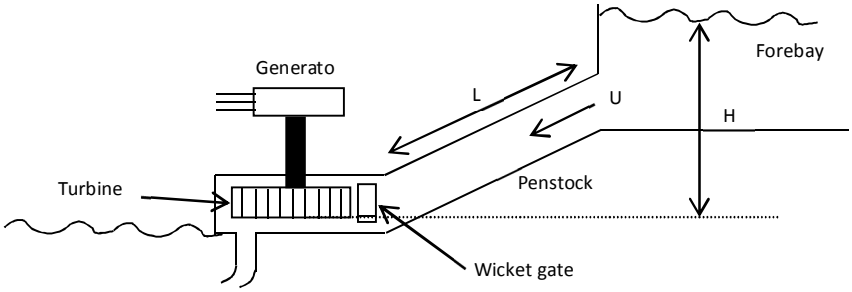

Figure (3.24) Schematic of hydroelectric plant

The velocity of water in the penstock is given by:

Where U = water velocity

$$U = K_U G \sqrt{H}$$

G = gate position

H = hydraulic head at gate

K_u = a constant of proportionality.

For small displacements about the operating point,

$$\Delta U = \frac{\partial U}{\partial H} \Delta H + \frac{\partial U}{\partial G} \Delta G \tag{3.48}$$

Substituting the appropriate expressions for the partial derivatives and dividing through by initial values

$U_0 = K_U G_0 \sqrt{H_0}$ yields, (3.49)

$$\frac{\Delta U}{U_0} = \frac{\Delta H}{2 H_0} + \frac{\Delta G}{G_0} \tag{3.50}$$

or

$$\frac{\Delta P_m}{P_{m0}} = \frac{\Delta H}{H_0} + \frac{\Delta U}{U_0} \tag{3.51}$$

where, the super bar denotes normalized values based on steady state operating values.

The turbine mechanical power is proportional to the product of pressure and flow; hence,

$P_m = K_p HU$

(3.52)

Linearizing by considering small displacements, and normalizing by dividing both sides by $P_{m0} = K_p H_0 U_0$,we have

$$\Delta \overline{U} = \tfrac{1}{2} \Delta \overline{H} + \Delta \overline{G} \tag{3.53}$$

$$\Delta \overline{P_m} = \Delta \overline{H} + \Delta \overline{U} \tag{3.54}$$

Or

Substituting for $\Delta\overline{U}$ from the previous equation yields,

$$\Delta \overline{P_m} = 1.5 \Delta \overline{H} + \Delta \overline{G} \tag{3.55}$$

$$\Delta \overline{P_m} = 3 \Delta \overline{U} - 2 \Delta \overline{G}$$

Alternatively, by substituting for $\Delta\overline{H}$, we may write (3.56)

The acceleration of water column due to a change in head at the turbine, characterized by Newton's second law of motion, may be

$$(\rho LA)\frac{d\Delta U}{dt} = -A(\rho a_g)\Delta H \tag{3.57}$$

expressed as

Where

L = length of conduit

A = pipe area

ρ = mass density

a_g= acceleration due to gravity

ρLA = mass of water in the conduit

$\rho a_g \Delta H$ = incremental change in pressure at turbine gate

t = time in seconds

By dividing both sides by $A\rho a_g H_0 U_0$, the acceleration equations in normalized form

$$\frac{LU_0}{a_g H_0}\frac{d}{dt}\left(\frac{\Delta U}{U_0}\right) = -\frac{\Delta H}{H_0} \tag{3.58}$$

becomes

$$T_W \frac{d\Delta\overline{U}}{dt} = -\Delta\overline{H} \tag{3.59}$$

Here $T_W = \frac{LU_0}{a_g H_0}$ is referred to as the water starting time. It represents the time required for the head H_0 to accelerate the water in the penstock from standstill to the velocityU_0.

We may now express the relationship between change in velocity and change in gate position as,

$$T_W \frac{d\Delta\overline{U}}{dt} = 2(\Delta\overline{G} - \Delta\overline{U}) \tag{3.60}$$

Replacing d/dt with the Laplace operator s, we may write

$$T_W s\Delta\overline{U} = 2(\Delta\overline{G} - \Delta\overline{U}) \tag{3.61}$$

Or

$$\Delta\overline{U} = \frac{1}{1 + \frac{1}{2}T_W s}\Delta\overline{G} \tag{3.62}$$

We recall that $\Delta\overline{U}$ in terms of $\Delta\overline{P_m}$ is given by

$$\Delta\overline{P_m} = 3\Delta\overline{U} - 2\Delta\overline{G} \tag{3.63}$$

Hence

$$\frac{\Delta\overline{P_m}}{\Delta\overline{G}} = \frac{1 - T_W s}{1 + \frac{1}{2}T_W s} \tag{3.64}$$

This is the classical transfer function of a hydraulic turbine. It shows how the turbine power output changes in response to a change in gate opening for an *ideal lossless* turbine.

3.13.2 Governors of Hydraulic Turbines

The basic function of the governor is to control speed and/or load. The primary speed/load control function involves speed error to control the gate position. In order to ensure satisfactory and stable parallel operation of parallel units, the speed governor is provided with droop characteristics, the purpose of which is to ensure equitable load sharing between generating units. Typically the droop is set at 5% which means that a speed change of 5% causes a 100% change in gate position, or power output. This corresponds to a gain of 1/0.05 or 20. We shall show however that such a simple governor (modeled by 1/R) is unsatisfactory. To demonstrate this argument, consider the governor turbine system shown below in figure (3.25).

The inertia constant of the generator is H and the machine is supplying an isolated load. Water starting time T_W is 2.0 and the damping constant is 0.0.

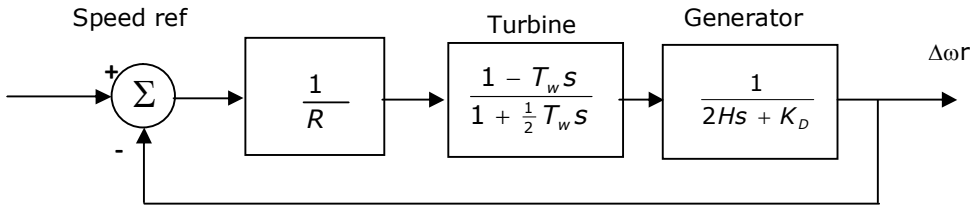

Figure (3.25) Governing system functional block diagram

The generator transfer function may easily be derived. Recall that the swing equation,

$$\frac{d\omega}{dt} = \frac{\pi f}{H}(P_m - P_e) \tag{3.65}$$

$$\frac{d\omega}{dt} = \frac{\pi f}{H}(P_m - P_e) + K_D\omega \tag{3.66}$$

If we add a damping term

For small changes

For an isolated load ΔP_e is zero. Also, normalizing the speed $\omega=2\pi f$, we get

$$\frac{d\Delta\omega}{dt} = \frac{\pi f}{H}(\Delta P_m - \Delta P_e) + K_D \Delta\omega \tag{3.67}$$

$$\frac{d\Delta\varpi}{dt} = \frac{1}{2H}\Delta P_m + K_D \Delta\varpi \tag{3.68}$$

Taking Laplace transforms,

$$s\Delta\varpi = \frac{1}{2H}\Delta P_m + K_D \Delta\varpi \tag{3.69}$$

and

$$\frac{\Delta\varpi}{\Delta P_m} = \frac{1}{2Hs + K_D} \tag{3.70}$$

An improvement in stability is achieved by including a transient droop R_T characteristic in addition to the normal permanent droop R.

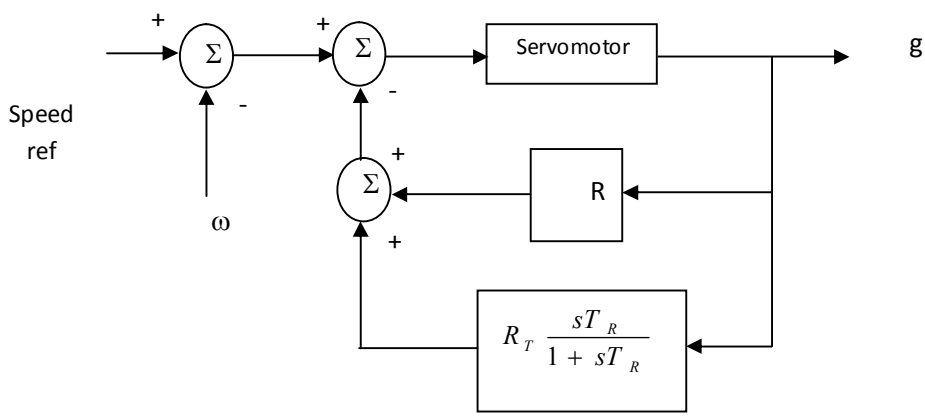

Figure (3.26) Governor with transient droop compensation

Because of the water starting time which is a result of water inertia, a change in the gate position will produce an initial turbine power change opposite to that required. For stable operation the gain should be transiently reduced to allow for water flow to catch up with the gate position. Hence the droop is transiently increased by adding R_T with a long resettling time T_R to the permanent droop R. If the change in gate

position is slow, only the effect of the low permanent droop which is kept within the normal range (0.05) need be considered.

3.13.3 PID Governors

Some electro-hydraulic governors are provided with three-term controllers with proportional-integral-derivative (PID) action, as shown below in figure (3.27) . These allow the possibility of higher response speeds by providing both transient gain reduction and transient gain increase. The derivative action is beneficial for isolated operation, particularly for plants with large water starting time (T_W = 3 s or more). Typical values are K_P = 3.0, K_I = 0.7 and K_D = 0.5. However the use of a high derivative gain or transient gain causes excessive oscillations and possibly instability when the generating unit is strongly connected to an interconnected system. Therefore, the

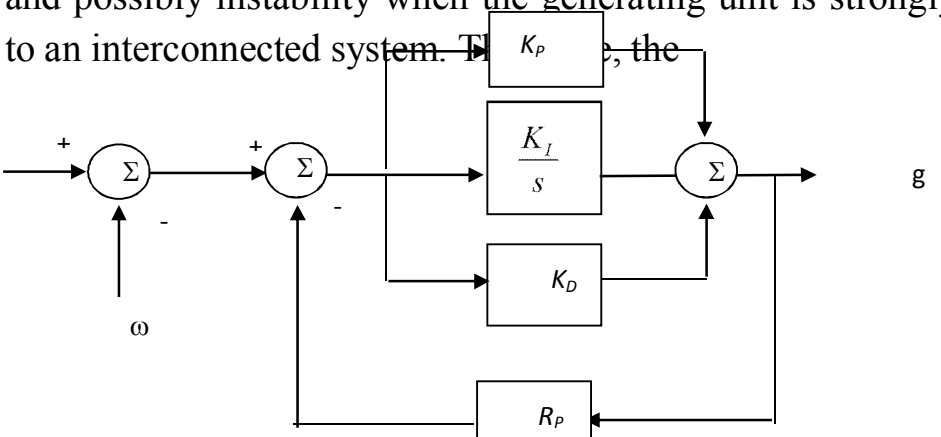

Figure (3.27) PID Governor controller

derivative gain is usually set to zero; without the derivative action, the transfer function of the PID (now PI) governor becomes

$$\frac{1}{R_P} \cdot \frac{1 + sK_P / K_I}{1 + s \cdot (1/R_P + K_P)/K_I}$$

3.13.4 Steam Turbines

A steam turbine converts stored energy of high pressure and high temperature steam into rotating energy, which is in turn converted into electrical energy by the generator. The steam is generated by boiling water using heat produced by a nuclear reactor or a furnace fired by fossil fuel (coal, oil or gas). Steam turbines usually consist of two or

more turbine sections coupled in series. Each turbine section consists of a set of moving blades attached to the rotor and a set of stationary vanes or nozzles.

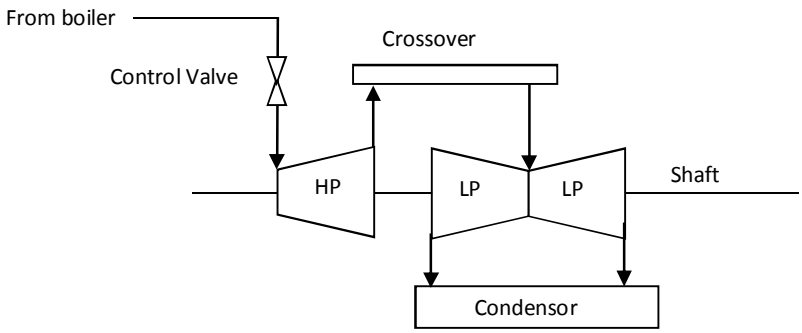

Figure (3.28) Steam Turbine Block Diagram

Depending on turbine configuration, fossil-fuelled units consist of high pressure (HP), intermediate pressure (IP), and low pressure (LP) turbine sections. They may be of either the reheat or non-reheat type. In a reheat type the steam leaving the HP section returns to the boiler for reheating before returning to the IP section. This improves efficiency. The steam exhausted from the turbine is expanded to sub atmospheric pressure and condensed in a condenser before returning to the boiler to repeat the cycle.

3.13.5 Steam Vessel Modeling

In the following we derive the transfer function of a steam vessel;

Figure (3.29) Steam Vessel Modeling

The continuity equation for the vessel is

$$\frac{dW}{dt} = V\frac{d\rho}{dt} = Q_{in} - Q_{out} \tag{3.71}$$

Where

W = weight of steam in vessel (kg)

= Vρ

V = Volume of vessel (m^3)

ρ = density of steam (kg/m^3)

Q = steam flow rate (kg/s)

t = time

Assuming the flow of the vessel to be proportional to the pressure in

$$Q_{out} = \frac{Q_0}{P_0}P$$

the vessel,

Where

P = pressure of steam in vessel (kPa)

P_0 = rated pressure

Q_0 = rated flow out of vessel

With constant temperature in vessel

$$\frac{d\rho}{dt} = \frac{dP}{dt}\frac{\partial\rho}{\partial P}$$

The change in density of steam with respect to pressure (∂ρ/∂P) at a given temperature may be determined from steam tables.

Our continuity equation thus becomes

$$\begin{aligned} Q_{in} - Q_{out} &= V\frac{\partial\rho}{\partial P}\frac{dP}{dt} \\ &= V\frac{\partial\rho}{\partial P}\frac{P_0}{Q_0}\frac{dQ_{out}}{dt} \end{aligned} \tag{3.72}$$

And in n Laplace form,

$$Q_{in} - Q_{out} = T_V sQ_{out} \tag{3.73}$$

Or

The time constant $T_V = V \frac{\partial \rho}{\partial P} \frac{P_0}{Q_0}$

$$\frac{Q_{out}}{Q_{in}} = \frac{1}{1 + T_V s} \tag{3.74}$$

3.13.6 Torque Developed by a Steam Turbine Stage

In modern steam turbines the force on each rotor blade, and hence the turbine torque, is proportional to the steam flow rate. Thus,

$T_m = kQ$, where k is a proportionality constant.

Valve Characteristics:

The control valves are usually of the plug-type with characteristics as shown below [2] in figure (3.30)

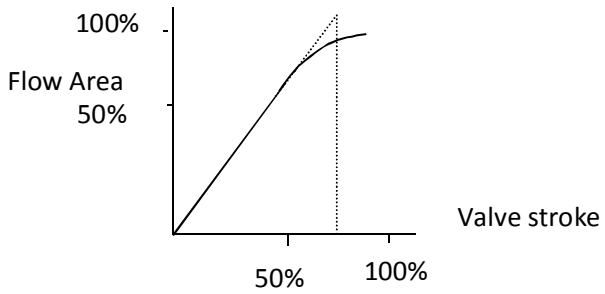

Figure (3.30) control valves characteristics of the plug-type

A block diagram representation of a steam turbine system is shown below in figure (3.31)

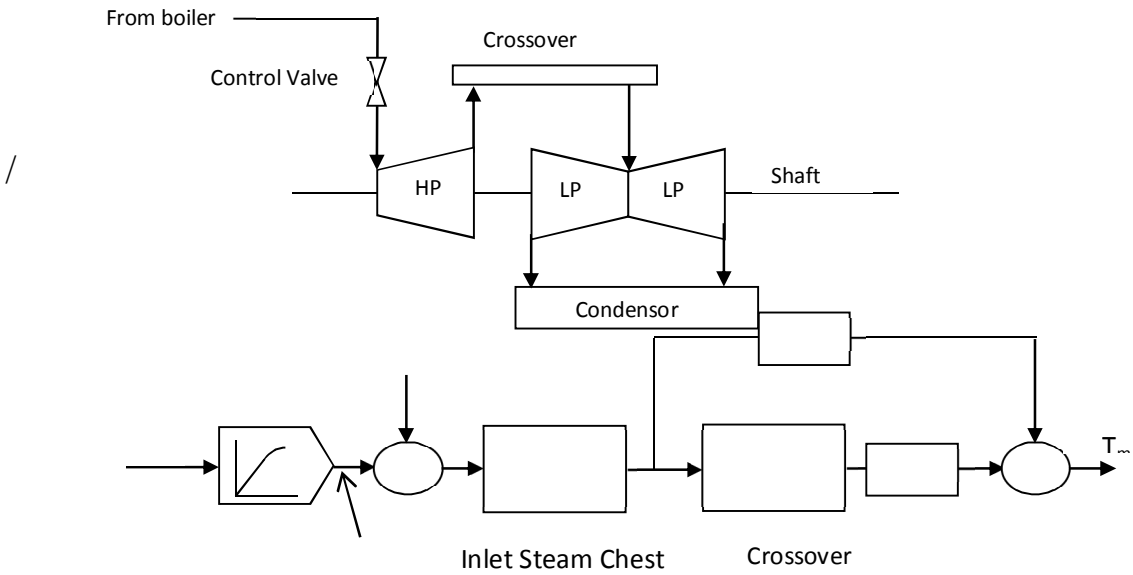

Figure (3.31) A block diagram representation of a steam turbine system

From figure above, a simplified transfer function may be derived as follows

$$\frac{\Delta T_m}{\Delta V_{CV}} = \frac{F_{HP}}{1+sT_{CH}} + \frac{1-F_{HP}}{(1+sT_{CH})(1+sT_{CO})} = \frac{1+sF_{HP}T_{CO}}{(1+sT_{CH})(1+sT_{CO})} \tag{3.75}$$

In deriving the above transfer function, it was assumed that the control valve characteristics are linear.

Control measures at the transmission system level include use of reactive compensation and transformer tap changers to regulate voltage. Voltage regulation improves system performance by preventing voltage collapse and increasing line loadability. Modern power systems apply power electronics to achieve fast compensation. Here below is a description of static var compensators which provide reactive compensation as needed by automatically switching on or off capacitive or inductive compensation.

3.14 Static VAR Compensator (SVC)

A Static VAR Compensator (SVC) is a fast acting Flexible AC Transmission Systems (FACTS) shunt device that uses power electronics to control reactive power flow and improve transient stability and power quality in power grids. SVCs mainly maintain voltage at a prescribed level by controlling the amount of reactive power injected into or absorbed from the power system at their coupling points. The device automatically switches between generating reactive power in capacitive mode when system voltage is low and absorbing reactive power in inductive mode when system voltage is high [7]. The operation of SVCs is achieved by switching capacitor banks on and off and by controlling or switching reactors connected on the secondary side of a coupling transformer. The configuration of an SVC is always mandated by the purpose of its use. Uses of SVCs include voltage control and stability, reactive power control, damping of power oscillations, reduction of transmission losses and increasing transmission capacity [8].

High maintenance older dynamic (as opposed to static) compensation schemes such as synchronous compensators are slower, more expensive and less reliable than SVCs.

3.14.1 SVC Characteristics

The figure (3.32) below shows a single-line diagram of a static VAR compensator and a simplified block diagram of its control system. Control branches configurations can, for example, comprise a TCR/ filter combination, i.e. a ThyristorControlled Reactor (TCR) for injection of linear inductive reactive power, and filter for fixed capacitive reactive power injection and harmonics filtering. Two other configurations are, Thyristor Switched Capacitors (TSC) and Thyristor Switched Reactors (TSR)

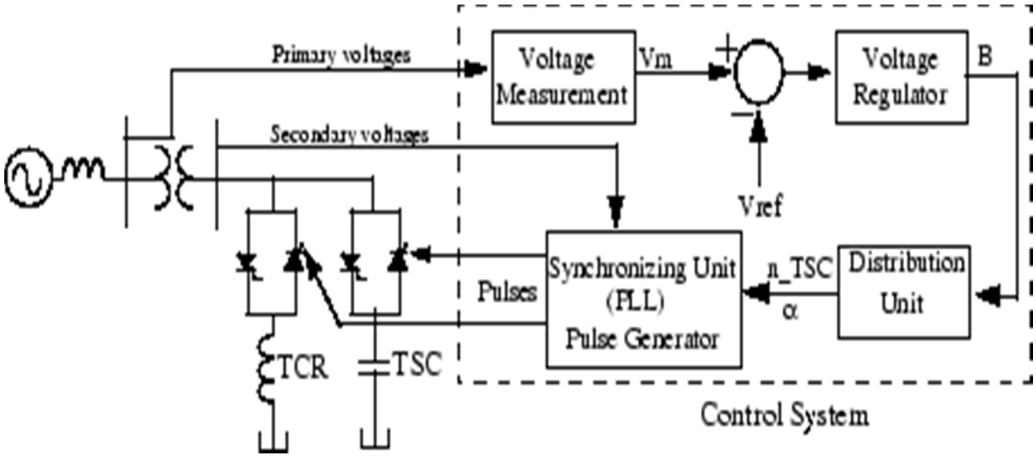

Figure (3.32) Simplified block diagram of SVC control system

Single-line Diagram of an SVC and Its Control System Block Diagram

The near-instantaneous operation of SVCs makes it possible to provide needed reactive power fast enough to prevent voltage collapse caused by reactive power demands in excess of system reserve, hence preventing partial or complete collapse of the system as well as improving post-disturbance power flow.

SVCs can be operated in two different modes:

- Voltage regulation mode, where the voltage is regulated within limits as explained below
- VAR control mode, where the SVC susceptance is kept constant.

When the SVC is operated in voltage regulation mode, the following applies,

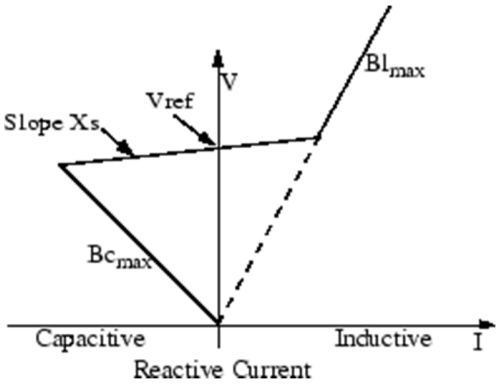

Figure (3.33) The V-I Characteristic Curve of SVC

As long as the SVC susceptance B stays within the maximum and minimum values imposed by the total reactive power of the capacitor

banks (Bc_{max}) and reactor banks (B_{lmax}), the voltage is regulated at the reference voltage V_{ref}. However, a voltage droop, usually between 1% and 4% at maximum reactive power output, is normally used and the V-I characteristic has the slope indicated in the figure above and is described by the following three equations[9]

$$V = Vref + Xs \cdot I \quad \text{SVC is in regulation range } (-Bc_{max} < B < Bl_{max}) \tag{3.76}$$

$$V = -\frac{I}{Bc_{max}} \quad \text{SVC is fully capacitive } (B = Bc_{max}) \tag{3.77}$$

$$V = \frac{I}{Bl_{max}} \quad \text{SVC is fully inductive } (B = Bl_{max}) \tag{3.78}$$

Where,

V Positive sequence voltage (pu)

I Reactive current (pu/Pbase) (I > 0 indicates an inductive current)

Xs Slope or droop reactance (pu/Pbase)

B_{cmax} Maximum capacitive susceptance (pu/Pbase) with all TSCs in service, no TSR or TCR

B_{lmax} Maximum inductive susceptance (pu/Pbase) with all TSRs in service or TCRs at full conduction, no TSC

Phase Three-phase base power specified in the block dialog box

CHAPTER FOUR

ANALYSIS of SUDAN NATIONAL GRID BEFORE and AFTER MEROWE DAM

4.1 Introduction

In this chapter the Sudanese Grid is examined and analyzed before and after the implementation of the Merowe Dam Project. The purpose of the analysis is to determine the impact of the implementation of the project (Merowe) on the performance of the Grid. The steady state behavior of the national Grid after incorporating the generation capacity of Merowe as well as system response disturbances such as short circuits, loss of any system element and other major insults are determined by performing load-flow, short circuit, contingency and transient stability analysis. This behavior is compared to how the Grid behaved before Merowe and the impact of Merowe is subsequently determined. In addition to broadening customer base, the added capacity from Merowe is expected to improve steady state and transient stability, reliability and control. Evidence of such improvement is investigated below.

Load-flow or power-flow analysis which is described in details in the next section, is used to examine the behavior of an electric network when steady state conditions are met. These conditions are:

a. Generation meets the load demand
b. Generators operate within their real and reactive power limits
c. Transformers and transmission lines are not overloaded
d. Bus voltages are at or very close to rated values

Short circuit analyses are performed to examine network response to short circuits such as three-phase to ground short circuit incidents. In such analysis it is desired to determine the short circuit current amount. The short circuit current amount, which is a function of the impedance of the network as seen from fault location, is calculated by dividing the pre-fault voltage level at the fault location by the impedance as seen

from the fault location. This current amount is used for such applications as assessing adequacy of insulation, ratings of new circuit elements and protective relay setting and coordination.

Contingency analysis examines impact on the system when one element such as a generating unit, a transformer or a transmission line is lost [9]. Networks are supposed to handle the loss of any one element without loss of stability. Some multiple contingencies are also expected to be tolerated by network.

Transient stability analysis is concerned with systems response to sudden large disturbances as opposed to the gradual change from one operating point to the next that characterizes steady state conditions. A power system satisfies transient stability criteria when it has the ability to acquire a new steady state operating point after a large sudden disturbance without losing synchronism. A large disturbance can for example be the loss of significant generation, load, transmission line or a short circuit.

4.2 Load Flow Analysis Theoretical Background

The electrical engineer needs to perform Load Flow studies for a variety of purposes; most notable are;

(1) Planning extensions to the system; new generation sites, new transmissio lines and transformers.

(2) Projected load growth (load forecasts) impact on the system.

(3) Planning interconnection with other systems

(4) Studying various conditions on the system, e.g. the effect of peak and off- peak conditions on the system loading and voltage levels.

(5) Estimating reactive power compensation requirements for the system.

(6) Contingency analysis; i.e. the effect of probable outages on the system performance.

The main complication in load flow studies is that, unlike short circuit or stability analysis, the system loads are modeled as active and reactive power rather than impedances, since this representation reflects the system demand at any given conditions. The resulting equations used to calculate the system voltages are non-linear and are solved using numerical analysis methods [8].

The General Busbar

Consider a system consisting n busbars. A general busbar in the system may be described having a power generation $\mathbf{S_{Gi}}$ and a load $\mathbf{S_{Li}}$. The net power flow into the busbar is $\mathbf{S_i}$ such that $\mathbf{S_{Gi} - S_{Li} = S_i}$ (see figure (4.1) below)

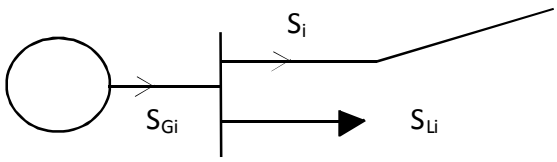

Figure (4.1) The General Busbar

Note that

$$\mathbf{S_{Gi} = P_{Gi} + j\,Q_{Gi}} \quad (4.1)$$

$$\mathbf{S_{Li} = P_{Li} + j\,Q_{Li}} \quad (4.2)$$

$$\mathbf{S_i = P_i + j\,Q_i} \quad (4.3)$$

It follows that

$$\mathbf{P_{Gi} - P_{Li} = P_i} \quad (4.4)$$

$$\mathbf{Q_{Gi} - Q_{Li} = Q_i} \quad (4.5)$$

Statement of the Power Flow Problem

Recall that the net power injected into any busbar I

$$S = P_i + jQ_i \quad (4.6)$$

$$= V_i I_i^*$$

The current I_i may be eliminated using the [Y] array.

[I] = [Y] • [V]

$$\boldsymbol{I_i = y_{i1} V_1 + y_{12} V_2 + \ldots\ldots + y_{1n} V_n} \qquad (4.7)$$

$$\text{or } \boldsymbol{I_i} = \sum_{j=1}^{n} \boldsymbol{y_{ij} V_j} \qquad i=1,2,\ldots\ldots\ldots,n$$

$$\boldsymbol{I_i} = \sum_{j=1}^{n} y_{ij} V_j \angle \psi_{ij} + -\delta_j \qquad i=1,2,\ldots\ldots\ldots,n$$

$$\boldsymbol{I_i^*} = \sum_{j=1}^{n} y_{ij} V_j \angle -\psi_{ij} - \delta_j \qquad i=1,2,\ldots\ldots\ldots,n \qquad (4.8)$$

Thus

$$\boldsymbol{S_i} = \boldsymbol{V I_i^*} = \sum_{j=1}^{n} V_i V_j y_{ij} \angle \delta_i - \psi_{ij} - \delta_j \qquad i=1,2,\ldots\ldots\ldots,n \qquad (4.9)$$

Separating into real and imaginary components

$$P_i = \sum_{j=1}^{n} V_i V_j y_{ij} \cos(\delta_i - \psi_{ij} - \delta_j) \qquad (4.10)$$

$$Q_i = \sum_{j=1}^{n} V_i V_j y_{ij} \sin(\delta_i - \psi_{ij} - \delta_j) \qquad (4.11)$$

Recall that

$$P_i = P_{Gi} - P_{LI} \qquad (4.12)$$

$$Q_i = Q_{Gi} - Q_{Li} \tag{4.13}$$

Hence,

$$P_{Gi} - P_{Li} = \sum_{j=1}^{n} V_i V_j y_{ij} \cos(\delta_i - \psi_{ij} - \delta_j) \tag{4.14}$$

$$Q_{Gi} - Q_{Li} = \sum_{j=1}^{n} V_i V_j y_{ij} \sin(\delta_i - \psi_{ij} - \delta_j) \tag{4.15}$$

At each bus-bar we are concerned with six variables;P_{Gi} ,Q_{Gi}, P_{Li}, Q_{Li}, V_i and δ_I .

Two are specified (P_{Li} and Q_{Li}), leaving P_{Gi} ,Q_{Gi}, P_{Li}, Q_{Li}, V_i and δ_i . The two power equations above must be satisfied, forcing two more variables to be satisfied to be able to solve the problem. As far as mathematics is concerned, *any* two variables may be specified; however, when the physical system is considered, we realize that the variables specified depend on the type of busbar of ***i***. We then find that we have three options summarized in the table below, with number of buses of each type per system or study is indicated in the last column.

Table 4.1 Statement of the Power Flow Problem

Bus Type	***Knowns***	***Unknowns***	***Approximate Number***
Slack	$V_i=1.0$ δ_i	P_{Gi} Q_{Gi}	*1*
Load	P_{Gi} Q_{Gi}	V_i δ_i	*~85%*
Generator	P_{Gi} V_i	δ_i Q_{Gi}	*~15%*

The first type is known as the slack, or reference bus. It is essentially a generator bus with no power constraints. It is necessary in any a.c circuit that one phasor quantity be selected as a reference. The slack busbar is selected for this purpose and its phase angle is set to zero and voltage magnitude to 1.0 p.u. It is common practice to select the generator with highest capacity as the slack bus.

The second type is the load bus. This applies to any bus where $P_{Gi}$and$Q_{Gi}$are known, but typically the sum of P_{Gi}= sum of $Q_{Gi} = 0$.That is to say that the total power, real or reactive entering any load bus equals the power leaving that bus. At such busbars the system equations are solved to find $V_i$and δ_i .

Generator busbars are sometimes called voltage controlled busbars, since the voltage is fixed at a specified value (by action of the A.V.R). The real power generation P_{Gi} is also fixed (by the governor-turbine setting). In this type of busbar the reactive power generation Q_{Gi} is unknown. However Q_{Gi} should not be allowed to exceed its limits Q_{Gimax} or Q_{Gimin} .If during problem solution Q_{Gi} is above or below its limits we set it at the appropriate limit and change the busbar type to a load busbarsince now both P_{Gi} and Q_{Gi} are specified.

The load flow problem may now be specified as follows:

Solve for the unknown variables using the known variables as listed in Table 2 for a system of known admittance matrix **[Y]**respecting reactive power limits on generators and the given loading condition. Additionally solve for the power flows on all lines and transformers.

Mathematically the problem is non-linear and can only be solved using numerical techniques. A method well suited to the load flow problem is the Newton-Raphson Method.

4.3 Grid Analysis

For this study two NEPLAN files were prepared; one is a model of the Grid before, and the other is a model of the Grid after Merowe. NEPLAN is used to perform power flow, contingency, short circuit and stability analyses on both models. Later the results obtained

are examined to determine the impact of the implementation of Merowe on the Grid.

The general purpose of load flow studies is to confirm that the scenarios considered under normal (no fault) conditions present no limit violations. This means that generators are not exceeding active or reactive power limits, voltages at all buses are within the admissible range (typically ± 5% of rated values) and that no transmission line or transformer is overloaded. High and low bus voltage conditions can be improved by connecting or disconnecting reactive or capacitive compensators as seen in the example above.

The purpose of N-1 contingency analyses is to check whether the loss of any one element such as a line, transformer or generator causes another element to be overloaded or lost due to any violation. If the system does not meet the N-1 criteria, i.e. it is found that loss of a particular element(s) causes a violation, measures should be taken to eliminate or mitigate the violation.

Short circuit analysis is carried out for the purpose of determining whether or not protective devices are rated in consistency with expected maximum fault currents. Proper operation of protective circuitry is vital to network transient stability and safe recovery from contingency especially when network elements are operated close to their limits.

Small signal stability analysis concern is the network behavior under small disturbances that are inherent to power networks while the concern of transient stability analysis is network behavior after being subjected to major disturbances.

The base case for the Before-Merowe analysis was modeled using 2008 (the year before commissioning of Merowe) system data. In other words, base case generation and load data, transmission line and transformer parameters and the topology of the network accurately represent the situation of the Sudanese electric network shortly before Merowe. The basecase also represents the peak demand/generation for the year 2008.

The basecase data and load flow results are labeled and presented in the appendix. It should be noted here that load data represents the load after shedding. The maximum available generation could not meet the total demand forcing the supply to be cut from some customers.

The performance of the grid at off-peak demand was examined by entering load data corresponding to these situations according to 2008 data. The data and results are presented in the Appendix, including use of reactive power compensation. As mentioned earlier, compensation is used to enhance performance of power systems by regulating voltage and increasing line loadability when needed.

Operation during high load conditions would generally requireRosaries plant to be operated at full capacity and all steam units of thermal plants would be operated close to their maximum output.During low load Rosaries plant would be operated at half to sixty percent capacity with additional power from some thermal units.

For the After-Merowe case high load conditions may requireMerowe plant to be operated at full capacity with all available thermal units operating at full or close to full capacity. While at low demand period

Merowewould be operated well below full capacity with most thermal unitsout of service. Future increase in demand is likely to change generation scheduling and to require new generation plants to be added. The basecase for studying the Grid after Merowe is built from load data corresponding to 2011 peak demand and the corresponding maximum generation for the year. Load flow analyses are performed to determine the steady state condition of the system. Detailed results are labeled and presented in the Appendix.

For simulation purposes bus voltages are considered within limits if they differ from rated values by less than 10%. From system operation point of view a difference of 5% or less is desired. Detailed results list the voltages at each bus, making it possible to spot violations that are in the 5% or 10% zones. From these results it is seen that a number of buses violate voltage limits with HAS1 being the worst bus. Increasing compensation improved HAS1 voltage slightly but brought GAD1 and GAD3 to acceptable limits. Further increase in compensation did not help as simulation indicated. This finding stresses the fact that compensation elements need to be placed carefully at selected locations and their reactive power output needs to be suitable for the desired change. The low voltage at HAS1 persisted after several attempts to adjust generation allocation and transformer regulation indicating the need for reinforcement of the circuit at that location. This finding is consistent with changes in the Grid that are outside the time frame of this study including a new substation that HAS1 is now connected to.

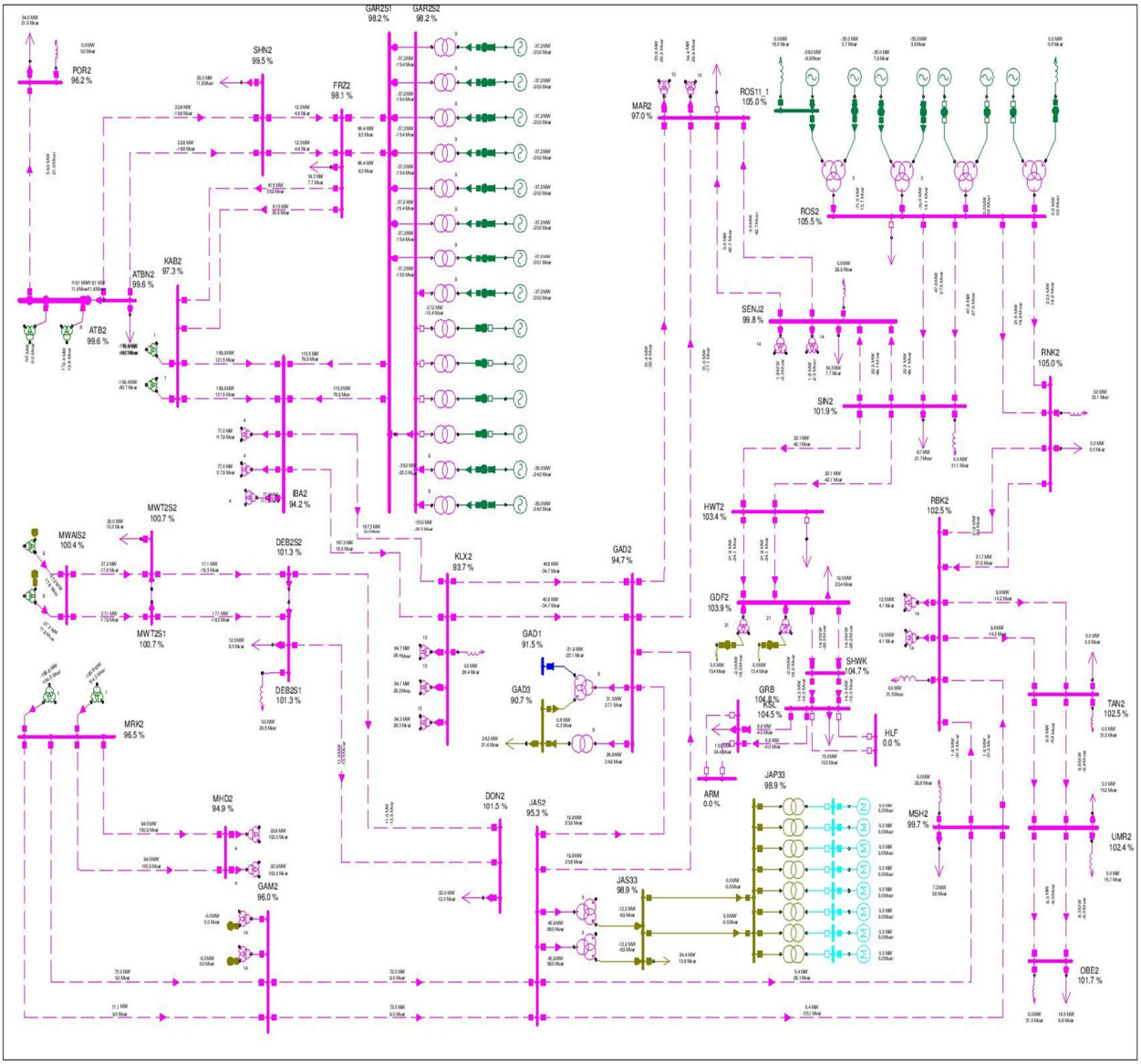
GAR2S1
98.2 %
GAR2S2
98.2 %
POR2
96.2 %
SHN2
99.5 %
FRZ2
98.1 %
MAR2
97.0 %
ROS11_1
105.0 %
ROS2
105.5 %
ATBN2
99.6 %
KAB2
97.3 %
ATB2
99.6 %
SENJ2
99.8 %
RNK2
105.0 %
SIN2
101.9 %
IBA2
94.2 %
HWT2
103.4 %
RBK2
102.5 %
MWT2S2
100.7 %
MWAIS2
100.4 %
DEB2S2
101.3 %
KLX2
93.7 %
GAD2
94.7 %
GDF2
103.9 %
GAD1
91.5 %
SHWK
104.7 %
GAD3
90.7 %
GRB
104.8 %
KSL
104.5 %
HLF
0.0 %
TAN2
102.5 %
MWT2S1
100.7 %
DEB2S1
101.3 %
MRK2
96.5 %
ARM
0.0 %
JAP33
98.9 %
MSH2
99.7 %
UMR2
102.4 %
MHD2
94.9 %
DON2
101.5 %
JAS2
95.3 %
JAS33
98.9 %
GAM2
96.0 %
OBE2
101.7 %

CHAPTER FIVE
CONCLUSIONS and RECOMMENDATIONS

5.1 CONCLUSIONS

The analyses presented in Chapter 4 are discussed here to determine the impact of Merowe on the Grid. The most obvious positive impact is the added capacity. Capacity increase ensures a wider base of industrial, commercial, governmental and residential customers is covered. Detailed discussion of the socioeconomic aspect of the impact of Merowe is beyond the scope of this thesis. The thesis is primarily concerned with the performance of the network in terms of stability.

The stability and proper steady state operation at high peak before Merowe could not be maintained without applying load shedding schemes because of generation and transmission capacities inadequacies. The need to shed loads has not completely been eliminated but has been greatly reduced. It is worth mentioning here that with generation and transmission capacity increase came an increase in demand.

The transmission capacity increase in the form of transmission overhead lines and transmission substations was mandated by the need to transfer the Merowe power to the load centers around the country. The design of the added transmission networks in general must take into consideration power transfer needs at the time of implementation as well as future growth. From the analysis above it is concluded that the performance of the single circuit line from Atbara to Port Sudan is poor. The introduction of the 500kv lines and substations for long distance transfer of power lead to the need to use compensation to regulate voltage. The performance of this circuit is satisfactory with proper compensation.

Future growth in demand will present challenges by bringing the network elements closer to limits. Economics of operation makes it impossible to maintain the redundancy in generation and transmission

capacities that used to characterize power networks in the past. This requires sophisticated power system operation including use of power electronics, fast acting controls and computer applications at the generation and transmission levels. One such application is the use of static var compensation at selected points in the network. As load conditions change compensation requirements change. Static var compensators automatically answer to those changing needs at high speed, hence enhancing performance and preventing instability. Smart allocation and dispatch of resources is another important requirement of future operation of the Sudanese Grid.

Overall, it is concluded that the added generation and transmission capacities caused Sudanese Grid performance to improve in terms of steady state and transient stability, voltage profile and N-1 contingency criteria. In the above studies it was assumed that proper protection schemes are applied at all times protecting equipment and guarding stability by fast and selective clearing of faults and undesired conditions.

5.2 RECOMMENDATIONS

In light of the analysis presented in the previous discussion the following recommendations are made:

1. **Addition of Plants Similar to Merowe in Capacity**: Despite the many advantages of Merowe Plant such as supplying a large portion of the much needed power to meet the ever increasing demand, the sheer size of the plant compared to the other generation plants in the system is a big concern. The reason is that the possibility of losing Merowe at any instant of time constitutes a serious risk to the stability of the entire network. It is therefore necessary to incorporate into the system at other locations, generation plants that are similar in capacity to Merowe.

2. **Increasing Generation in Khartoum Area**:Merowe and Rosairs, the two largest hydro generation plants are far from load centers. Thus transmission losses are significant and are affecting the stability of the network. Consequently it is recommended that Khartoum area generation be increased; especially that Khartoum is the largest power consumer using up to 60% of the total generation capacity.
3. **Addressing Future Generation Shortages**: Power usage increases by more than 12% annually and this figure is expected to rise even further. The excess generation capacity resulting from Merowe Project will not last more than a few years due to this rapid increase in power consumption. Therefore it is recommended that power generation should increase in proportion to the expected increase in demand to avoid shortages. This of course means building more power plants.
4. **Addition of SVCs to the System**: Load flow and stability studies indicate a need to add SVC units to improve upon the network. It is recommended that these units be installed in accordance with detailed studies to determine unit size and location.
5. **Increasing Capacity of System Components**: The study revealed the negative impact of load increases on system components. It is recommended that in order to maintain N-1 security criteria for system components the capacity of those components be adequately increased. Without N-1 security measures continuity and stability of supply will be negatively impacted thus affecting consumers.
6. **Fault Level Studies**: The addition of generation capacity to meet the increasing demand will change fault current levels in the system, especially in Khartoum area where more generation should be added. This requires carrying out system-wide fault studies paying special attention to Khartoum area.

References

[1] Hadi Saadat “Power System Analysis” ,WCB McGraw-Hill International Editions ,1999.

[2] WILLIAM D. STEVENSON "ELEMENTS OF POWER SYSTEM ANALYSIS" 1982- MC

[3] P M Anderson and A A Fouad "POWER SYSTEM CONTROL and STABILITY" Science Press, Ephrata, 1980

[4] Jan Machowski and Janusz W.Bialek and James R.Bumby "POWER SYSTEM DYNAMICS Stability and Control" John Wiley and Sons, Ltd , 2008

[5] Mohamed E El-Hawary "Electric Power System Analysis and Control" John Wiley and Sons , Toronto , 2003

[6] P. KUNDUR "POWER SYSTEM STABILITY and CONTROL" John Wiley and Sons ,Ontario ,1994

[7] Robert H.Miller and James H.Malinowski 'POWER SYSTEM OPERATION' McGraw-Hill , New York , 1994

[8] J Arrillaga and N R Watson "COMPUTER MODELLING OF ELECTRICAL POWER SYSTEMS" John Wiley and Sons, Ltd. New York, 2001

[9] John J. Grainer and William D. Stevenson, JR "POWER SYSTEM ANALYSES" Tata McGraw- Hill , North Carolina , 2005

Table 1.1: Before-Merowe Basecase Load

BusName	Descriptin	MW	Mvar
ATBN2	LO-Atbara (NEC)	13.6	11.8
BAG1	LO-El Bager	19.1	8.8
BAG1	L-1229758974	16.9	6.7
BNT1	LO-Banat	0	0
FAO1	LO-El Fau	6.8	3.1
FAR1	LO-Farok	82.1	38
GAD2	GAD-220	16.4	-40
GAD3	LO-Giad	10	7
GBA_6	LO-El Girba	0	0
GDF66	LO-Geradef	0	0
HAG1	LO-Hag Abdallah	3.3	1.6
HAS1	LO-Hassa Heisa	26.1	13.8
IBA1	LO-Eid Babiker	18.2	11.6
IBA1	L-1229758958	18.2	11.6
IZG1	LO-Izergab	39.5	22.7
JAS2	L-1229758950	10.2	3.5
JAS33	LO-Jebel Aulia	18	7.9
KHE1	LO-Karthum East	84.8	35.3
KHN3	LO-KHN	14.8	6.7
KL366	LO-Kilo 3	0	0
KLX1	LO-Kilo X	10.2	4.7
KLX1	L-1229758966	9	5.3
KSL11	LO-Kassala	0	0
KUK1	LO-Kuku	55.4	28.9

KUK3	LO-KUK	34.2	12
MAN1	LO-Managil	8.6	3.9
MAR1	LO-Meringan	54.5	18.2
MHD1	LO-Mahadia	28.5	15
MHD2	L-1229758942	43.4	20
MNA1	LO-Mina Sharif	14	6.4
MSH2	LO-Mashkur	10	4.8
MUG1	LO-Mugran	96	50.5
NHLF66	LO-Halfa	0	0
OMD1	LO-Omdurman	43.7	26.6
ROS2	LO-Roseires	4.5	2.5
RWS66	LO-Rawesda	0	0
SENJ1	LO-Sennar	30	8.1
SENP1	LO-Sennar Hydro	12.3	5.2
SHG1	LO-Shagara	59.6	24.2
SHN2	LO-Shendi	6.9	4.9
	Total	918.8	391.3

Table 1.2: Before-Merowe Basecase Generation

BusName	Description	Type	MW	Mvar
JAP69_1	Jebel Aulia Hydro G1	Asynchronous	-3.8	2.355
JAP69_2	Jebel Aulia Hydro G2	Asynchronous	-3.8	2.355
JAP69_3	Jebel Aulia Hydro G3	Asynchronous	-3.8	2.355
JAP69_4	Jebel Aulia Hydro G4	Asynchronous	-3.8	2.355
JAP69_5	Jebel Aulia Hydro G5	Asynchronous	-3.8	2.355
JAP69_6	Jebel Aulia Hydro G6	Asynchronous	-3.8	2.355
JAP69_7	Jebel Aulia Hydro G7	Asynchronous	-3.8	2.355
JAP69_8	Jebel Aulia Hydro G8	Asynchronous	-3.8	2.355
GAR_G1	Garri I G1	Asynchronous	-37.17	-16.308
GAR_G10	Garri II G7	Asynchronous	-37.17	-16.119
GAR_G11	Garri II G8	Asynchronous	-37.17	-16.119
GAR_G12	Garri II ST4	Asynchronous	-37.17	-16.119
GAR_G13	Garri IIII ST09	Asynchronous	-40	-19.585
GAR_G14	Garri IIII ST10	Asynchronous	-40	-19.585
GAR_G2	Garri I G2	Asynchronous	-37.17	-16.308
GAR_G3	Garri I ST1	Asynchronous	-37.17	-16.308
GAR_G4	Garri I G3	Asynchronous	-37.17	-16.308
GAR_G5	Garri I G4	Asynchronous	-37.17	-16.308
GAR_G6	Garri I ST2	Asynchronous	-37.17	-16.308
GAR_G7	Garri II G5	Asynchronous	-37.17	-16.401
GAR_G8	Garri II G6	Asynchronous	-37.17	-16.119
GAR_G9	Garri II ST3	Asynchronous	-37.17	-16.119
KHN11_GT_4	KN GT4	Asynchronous	-17	-10.6
KHN11_GT1	KN GT1	Asynchronous	-17	-3.428
KHN11_ST1	KN ST1	Asynchronous	-30	-20.143
KHN11_ST2	KN ST2	Asynchronous	-30	-20.143
KHN11_ST3	KN ST3	Asynchronous	-60	-37.852
KHN11_ST4	KN ST4	Asynchronous	-60	-37.852
KHN11_ST5	KN ST5	Asynchronous	-110	60
KHN11_ST6	KN ST6	Asynchronous	-110	60
ROS11_1	Roseires G1	Asynchronous	9.797	-43.319
ROS11_2	Roseires G2	Asynchronous	6.078	-16.616
ROS11_3	Roseires G3	Asynchronous	10.139	-27.716
ROS11_4	Roseires G4	Asynchronous	6.29	-17.196
ROS11_5	Roseires G5	Asynchronous	10.139	-27.716
ROS11_6	Roseires G6	Asynchronous	6.29	-17.196
ROS11_7	Roseires G7	Asynchronous	6.048	-6.334
SENP11_1	Sennar G1	Asynchronous	-7.5	-5
SENP11_2	Sennar G2	Asynchronous	-7.5	-5
Total			-950.659	-391.285

Table: 1.3 Before-Merowe Basecase Load flow

BusName	VoltageLevel	% of RatedVoltagw	MW	Mvar
ATB2	224.186	101.9	0	0
ATBN2	224.155	101.89	13.6	11.8
BAG1	103.47	94.06	36	15.5
BNT1	0	0	0	0
FAO1	107.495	97.72	6.8	3.1
FAR1	104.776	95.25	82.1	38
FRZ2	217.705	98.96	0	0
GAD1	103.73	94.3	0	0
GAD2	207.131	94.15	16.4	0
GAD3	31.109	94.27	10	7
GAM1	107.526	97.75	0	0
GAM2	202.973	92.26	0	0
GAM3_1	32.259	97.76	0	0
GAM3_2	32.259	97.76	0	0
GAR2S1	218.143	99.16	0	0
GAR2S2	218.306	99.23	0	0
GDF1	108.939	99.04	0	0
HAG1	108.626	98.75	3.3	1.6
HAS1	102.213	92.92	26.1	13.8
IBA1	108.278	98.43	36.4	23.2
IBA2	210.95	95.89	0	0
IBA3_1	32.377	98.11	0	0
IBA3_2	32.377	98.11	0	0
IZG1	106.298	96.63	39.5	22.7
JAP33	33.32	100.97	0	0
JAS1	107.936	98.12	0	0
JAS2	204.298	92.86	10.2	3.5
JAS33	33.429	101.3	18	7.9
KAB2	215.736	98.06	0	0
KHE1	106.038	96.4	84.8	35.3
KHN1	106.912	97.19	0	0
KHN3	34.233	103.74	14.8	6.7
KLX1	105.824	96.2	19.2	10
KLX11_1	10.576	96.14	0	0
KLX11_2	10.576	96.15	0	0
KLX11_3	10.576	96.15	0	0
KLX2	209.147	95.07	0	0
KUK1	106.267	96.61	55.4	28.9
KUK11_1	11.389	103.54	0	0
KUK11_2	11.389	103.54	0	0
KUK11_3	11.389	103.54	0	0
KUK3	34.186	103.59	34.2	12
MAN1	107.267	97.52	8.6	3.9
MAR1	108.311	98.46	54.5	18.2
MHD1	105.936	96.31	28.5	15
MHD2	200.186	90.99	43.4	20
MHD3_1	31.742	96.19	0	0
MHD3_2	31.742	96.19	0	0
MNA1	105.113	95.56	14	6.4

Table: 2.1 After-Merowe Basecase Load

BusName	Description	MW	Mvar
ATBN2	LO-Atbara (NEC)	70.9	46.3
BAG1	LO-El Bager	25.6	12.7
DEB2S1	LO-Debba	12	8
DON2	LO-Dongola	22	12
FAR1	LO-Farok	71.6	45.2
FRZ2	LO-FRZ2	34.3	7.7
GAD3	LO-Giad	26.2	21.6
GDF2	LO-GADAREF	19	22.4
GRB	LO-GIRBA	15	10.5
HAG1	LO-Hag Abdallah	10.8	14.2
HAS1	LO-Hassa Heisa	44.3	25.1
IBA1	LO-Eid Babiker	42.8	33.2
IZG1	LO-Izergab	55	34.6
JAS33	LO-Jebel Aulia	24.4	13.8
KHE1	LO-Karthum East	148.3	88.7
KLX1	LO-Kilo X	35.7	20.2
KSL	LO-KSL	13.5	24.4
KUK1	LO-Kuku	46.1	27.1
LOM1	LO-Local market	72.1	47.2
MAN1	LO-Managil	21.4	3.4
MAR1	LO-Meringan	28.1	14.3
MHD1	LO-Mahadia	108.3	64.9
MSH2	LO-Mashkur	7.2	3.8
MUG1	LO-Mugran	112	58.6
MWT2S2	LO-Merowe Town	20	10
OBE2	LO-El Obeid	16.5	8.8
OMD1	LO-Omdurman	113.5	71.2
POR2	LO-Port Sudan	54	21
RBK1	LO-Rabak	27.8	14.2
SENJ2	LO-SINJ-220	34.3	7.7
SHG1	LO-Shagara	83.6	60.9
SHN2	LO-Shendi	20	11.9
SIN2	LO-Singa 220	6.7	21.7
UMR2	LO-Umraba 220	3	15.2
	Total	1446	902.5

Table: 2.2 After-Merowe Basecase Generation

Name	Description	Type	MW	Mvar
GAR_G1	Garri I G1	synchronous	-37.17	-19.991
GAR_G13	Garri IIII ST09	synchronous	-35	-24.011
GAR_G14	Garri IIII ST10	synchronous	-35	-24.011
GAR_G2	Garri I G2	synchronous	-37.17	-19.991
GAR_G3	Garri I ST1	synchronous	-37.17	-19.991
GAR_G4	Garri I G3	synchronous	-37.17	-19.991
GAR_G5	Garri I G4	synchronous	-37.17	-19.991
GAR_G6	Garri I ST2	synchronous	-37.17	-19.991
GAR_G7	Garri II G5	synchronous	-37.17	-20.11
GAR_G8	Garri II G6	synchronous	-37.17	-19.98
GBA_6	El Girba pump 2	synchronous	-1.6	2.147
GBA_6	El Girba pump 1	synchronous	-1.6	2.147
GBA_6	El Girba Kap GT1	synchronous	-4	2.147
GBA_6	El Girba Diesel GT2	synchronous	-1.6	2.147
KHN11_GT1	KN GT1	synchronous	-17	-5.604
KHN11_ST5	KN ST5	synchronous	-55	42.718
KHN11_ST6	KN ST6	synchronous	-100	28.008
KSL11	Kassala G1-4	synchronous	0	0
MWP14_1	Merowe G1	synchronous	-63.736	-53.037
MWP14_2	Merowe G2	synchronous	-63.736	-53.037
MWP14_3	Merowe G3	synchronous	-110	-25.25
MWP14_4	Merowe G4	synchronous	-110	-25.287
MWP14_5	Merowe G5	synchronous	-110	-25.155
MWP14_6	Merowe G6	synchronous	-110	-25.23
MWP14_7	Merowe G7	synchronous	-110	-25.424
MWP14_8	Merowe G8	synchronous	-110	-25.449
ROS11_1	Roseires G1	synchronous	-36	-8.927
ROS11_2	Roseires G2	synchronous	-35	3.686
ROS11_3	Roseires G3	synchronous	-35	7.918
ROS11_4	Roseires G4	synchronous	-35	3.874
SENP11_1	Sennar G1	synchronous	-7.5	-5
SENP11_2	Sennar G2	synchronous	-7.5	-5
Total			-1491.632	-395.666

Table:2.3 After-Merowe Basecase Load Flow (Contd)

BusName	Voltage Level	% of Rated
ATB2	219.182	99.63
ATB3_1	32.864	99.59
ATBN2	219.18	99.63
BAG1	100.232	91.12
FAO1	105.578	95.98
FAR1	98.802	89.82
FRZ2	215.835	98.11
GAD1	100.631	91.48
GAD2	208.28	94.67
GAD3	29.919	90.66
GAM1	103.867	94.42
GAM2	211.122	95.96
GAM3_1	31.16	94.42
GAM3_2	31.16	94.42
GBA_6	6	100
GDF1	105.876	96.25
GDF11_1	11.777	107.06
GDF2	228.635	103.92
GDF3_2	31.241	94.67
GDF3_4	31.241	94.67
GDF66	68.569	103.89
GRB	230.521	104.78
HAG1	103.778	94.34
HAS1	94.758	86.14
HWT2	227.495	103.41
IBA1	105.171	95.61
IBA2	207.326	94.24
IBA3_1	31.429	95.24
IBA3_2	31.429	95.24
IZG1	102.679	93.34
JAP33	32.621	98.85
JAS1	104.856	95.32
JAS2	209.609	95.28
JAS33	32.621	98.85
KAB2	214.097	97.32
KAB3_1	31.96	96.85
KAB3_2	31.96	96.85
KAB5	459.686	91.94

BusName	Voltage Level	% of Rated
KHE1	100.009	90.92
KHN1	101.548	92.32
KHN3	33.91	102.76
KL366	67.727	102.62
KLX1	99.999	90.91
KLX11_1	9.99	90.82
KLX11_2	9.991	90.83
KLX11_3	9.991	90.82
KLX2	206.194	93.72
KSL	229.97	104.53
KUK1	100.551	91.41
KUK11_1	11.163	101.48
KUK11_2	11.163	101.48
KUK11_3	11.163	101.48
KUK3	33.458	101.39
LOM1	99.742	90.67
MAN1	102.576	93.25
MAR1	104.509	95.01
MAR11_1	10.425	94.78
MAR11_2	10.386	94.42
MAR2	213.493	97.04
MHD1	102.316	93.01
MHD2	208.713	94.87
MHD3_1	30.548	92.57
MHD3_2	30.548	92.57
MNA1	108.208	98.37
MRK2	212.311	96.51
MRK3_1	31.738	96.18
MRK3_2	31.738	96.18
MSH2	219.436	99.74
MUG1	99.443	90.4
MWAIS2	220.801	100.36
MWAIS3_1	33.16	100.49
MWAIS3_2	33.16	100.49
MWAIS5_S1	505.321	101.06
MWAIS5_S2	505.347	101.07
MWT2S1	221.463	100.66
MWT2S2	221.456	100.66
NHLF66	67.847	102.8
OBE2	223.686	101.68

Table: 2.3 After-Merowe Basecase Load Flow (Contd.)

BusName	Voltage Level	% of Rated
OMD1	100.289	91.17
POR2	211.724	96.24
RBK1	105.469	95.88
RBK11_1	10.543	95.85
RBK11_2	10.543	95.85
RBK2	225.479	102.49
RNK2	230.932	104.97
SENJ2	219.495	99.77
SENJ3	32.416	98.23
SENP1	107.915	98.1
SENP11_1	10.817	98.33
SENP11_2	10.817	98.33
SHG1	99.765	90.7
SHK66	68.041	103.09
SHN2	218.79	99.45
SHWK	230.329	104.69
SIN2	224.076	101.85
TAN2	225.549	102.52
TR3-IBAT3_33	31.429	95.24
UMR2	225.187	102.36
UMR2	225.187	102.36